İSTANBUL TECHNICAL UNIVERSITY ★ INSTITUTE OF SCIENCE AND TECHNOLOGY

CRASHWORTHY DESIGN OF A HELICOPTER CABIN FLOOR STRUCTURE

M.Sc. THESIS

İbrahim GÜNAL, B.Sc.

Department : MECHANICAL ENGINEERING

Programme: SOLID MECHANICS

MAY 2006

İSTANBUL TECHNICAL UNIVERSITY ★ INSTITUTE OF SCIENCE AND TECHNOLOGY

CRASHWORTHY DESIGN OF A HELICOPTER CABIN FLOOR STRUCTURE

M.Sc. Thesis by

İbrahim GÜNAL, B.Sc.

503031509

Date of submission : May 8, 2006

Date of defence examination: June 15, 2006

Supervisor (Chairman): Prof. Dr. Süleyman TOLUN

Members of the Examining Committee Prof.Dr. Zahit MECİTOĞLU

Prof. Dr. Mehmet H. OMURTAG

MAY 2006

Acknowledgements

I would like to express my gratitude to people who made possible to complete this study. I am grateful to my supervisor Professor Süleyman Tolun to rely on me and encouraged me to perform this study.

Also, many thanks to Serkan Us and Ahmet Kurt, from Bias Eng., for their software support and advices, to Hasan Ibacoglu for his creative designs and data supports and to other friends from ROTAM for their recommendations. I want to thank H. Gokmen Aksoy for his guiding ideas.

I am grateful to my parents for their patients and encouragements in every decisions of me through my career. Finally, thank you *moi xell*.

May 2006 **İbrahim GÜNAL**

HELİKOPTER KABİN ALTI YAPISININ DARBE SÖNÜMLEMEYE UYGUN TASARIMI

Özet

Mühendislik yapılarını oluşturan yapı elemanlarının düşük darbe hızlarındaki enerji sönümleme kabiliyetlerinin belirlenmesi ve bunların yapısal tasarımlara uygulanması çalışmaları günümüzde güncelliğini koruyan araştırma konularıdır. Düşük hızdaki darbe yükleri helikopterlerin uygunsuz inişleri esnasında zeminle olan çarpışmalarından tepki kuvvetleri olarak ortaya çıkabilir. Bu çalışmada bir helikopter modelinin uygunsuz iniş esnasında zeminle çarpışmasından doğan darbe enerjisini yapısal bütünlüğünü koruyarak sönümleyebilecek bir sandviç alt kabuk tasarımı üzerinde durulmuştur. Tasarımda yapının bütününde sandviç perde, enine ve boyuna destek elemanları ile alt kabukta oluşan tabaka ayrılması hasarı ve hasarın ilerleme şekli MSC.DYTRAN explicit sonlu elemanlar programında analiz edilmiştir. Ayrıca yerel olarak yapı elemanlarında oluşabilecek hasar tipleri analizden elde edilen veriler ışığında ayrı olarak ele alınmıştır. Tasarım kriteri olarak insan vücudunun düşey yöndeki ivmelenme limiti göz önünde bulundurulmuştur. Bu çalışmada elde edilen veriler ileriki tasarımlar için bir ön adım niteliğindedir.

CRASHWORTHY DESIGN OF A HELICOPTER CABIN FLOOR STRUCTURE

Abstract

Today it is very popular research subject to investigate low velocity impact crashworthiness capability of structural elements and applying resulting philosophies into engineering designs. Low velocity impact loads can be experienced in crush event of a helicopter with ground during improper landing situations. Through this paper a sandwich cabin-floor which absorbs the crush energy saving its structural integrity during crush event was examined. Onset of failure and delamination growth through laminates of bulkheads, transverse and longitudinal stiffeners and bottom plate were analyzed globally with MSC.DYTRAN explicit finite element code. Also local failure modes for sandwich structural elements were examined using outputs of analysis. The vertical acceleration/deceleration limits of human body were considered as design limit criteria. Result data from this study will be an important source for following designs of the helicopter cabin-floor.

TABLE OF CONTENTS

LIST OF TABLES

LIST OF FIGURES

LIST OF SYMBOLS

A	: Extentional stiffness
B	: First moment of area
C	: Compliance
D	: Flexural rigidity
D_o, D_f, D_c	: Flexural rigidity of components in a sandwich
E	: Modulus of elasticity
G	: Shear modulus
I	: Inertia moments
L	: Length of beam
M	: Bending moment
N	: Normal force (where subscripts are x,y)
N	: In plane force (where subscripts are 1,2)
N	: Shape functions
Q	: Point load/shear resultant force
S	: Shear stiffness
T	: Transverse force
U	: Strain energy, potential energy
W	**:** Weight, work
A, B, D	**:** Extention, coupling and bending stiffness matrices
Q	**:** Matrix of elastic constants
T	**:** Transformation matrices
a, b	**:** Sides of a rectangular panel
d	: Distance between centroids of sandwich facesheets
m, n	: Integers-summation, modes or exponents
q	: Distributed load
t	: Component thickness
u, v, w	: Deformation components
x, y, z	: Cartesian coordinate system
w_b, w_s	: Deformation due to bending and shear, respectively
ε	: Strain
ε_1	: Allowable direct strain in fibre direction
ε_2	: Allowable direct strain normal to the fibre (in-plane)
ε_6	: Allowable shear strain in 12-plane
θ	: Stress off-set angle measured from 1 axis
κ	: Curvatures
ν	: Poisson's ratio
σ_{ij}	: Stress components
σ_1	: Direct stress in fibre direction
σ_2	: Direct stress normal to the fibre (in-plane)
σ_6 or σ_{12}	: Shear stress in 12-plane

ψ	: Cross section rotations
ρ	**:** Density

Subscript

b	: Bending moment
c	: Component
cr	: Critical value
f	: Failure
s	: Shear component
t	: Tension
1, 2, 3	: Refer to the coordinate system
x, y, z	: Cartesian directions

Superscript

u	: Ultimate value
T	: Transpose of given matrix

1. INTRODUCTION

Sandwich structures have gained widespread acceptance in engineering structures because of their advantages of obtaining stiff, strong, durable structural elements in very light weights. Today composite sandwiches have been using in many applications such as marine, aerospace, automotive and space industry because of their high strength to weight ratio and energy absorbing capabilities. However; wide usage of these materials requires improved understanding of mechanical behavior of these materials under some extreme events such as crashes [1].

A typical sandwich consists of two high strength face-sheet materials filled with a low density core material in between. The American society for testing and materials (ASTM) defines a sandwich structure as follows:

"A structural sandwich is a special form of a laminated composite comprising of a combination of different materials that are bounded to each other so as to utilize the properties of each separate component to the structural advantage of the whole assembly."

As in common structures, in sandwich structures, generally, it is not so difficult to anticipate the behavior of member under certain loading conditions. But major problems appear in junction regions that assign boundary condition to the member and in the case of combined loadings. Because the orthotropy and more complicated material content, determining possible failure in this kind of structures is required more detailed analyses both in experimentally and numerically. Determining the failure attitude of such members both in locally and globally is more difficult in nature unlike isotropic media. Designing of a sandwich construction, therefore, can be considered in two stages. At first structural elements that are considered to be used in design are determined and tested to understand their individual behaviors under complex loading schemes. Then they are properly used in construction considering their characteristic behaviors.

Crash behavior of metallic materials can be modeled in FEA programs more realistically compared with composite materials. Because isotropic media has been examined so much and were generated many theories correlated with experiments so far. In the examining of large deformations of metallic structures there are many modeling tools. Because they deform plastically before rupture, some plastic constituent laws required to define each material behavior separately. But in composite structures it is more complex job modeling failure mathematically. Especially when the behavior of structure was forced to give certain trends such as like in sandwiches, then it brings some more problems with the philosophy of the structure.

When the loading conditions became more complex combined with material nonlinearity, it is being very hard job to predict failure attitude of structure. Therefore; detailed modeling of sandwich structures is limited because of many unknown parameters and complexity in complex physical events like crashes. Because in reality many failure modes such as fiber or/and matrix cracking, delamination and instability may possibly occur interactively. However; there are still insufficient failure models to analyze out-of-plane failure behavior of composites structures for delamination failure for example. That is why component based experiments are still needed. Failure can be predicted locally by the help of experimental data.

In the case of using sandwich structures in helicopter constructions, design of structure is also important to consider safety of pilots and other occupants because of less possibility to survive in the accident of rotary-wing aircrafts. Sandwich composites can only have an advantage decreasing the total weight of the structure. However it is an important fact that structures must be designed to supply sufficiently safe volume for pilot and occupants against crashes. Human body limits and nonstructural component behaviors such as seats must be considered in design. MIL-STD-1290A [2] gives a good design frame for a crashworthy design of structures.

Helicopter crash accidents with a high vertical impact velocity component, the crash loads have to be absorbed by controlled structural deformation, involving the landing gear, the sub-floor and seat system.

1.1 Background and Literature Survey

Prior to World War II sandwich concept was applied to panels in small planes, but the World War II Mosquito bomber, designed and built by Haviland Airplane Company, was the first structure to incorporate sandwich panels. The excellent performance demonstrated by this airplane had convinced numerous aircraft designers of the superiority of sandwich structure as a mean to construct more efficient airplanes. The structural efficiency of the concept was now generally accepted.

Figure 1.1 A Mosquito Bomber from World War II.

A lot of researches have been performed until today to develop more efficient core materials to decrease the weight of sandwich panels. Honeycomb core materials developed for the aerospace industry in the late 1940s. Today honeycomb cores are still mostly preferred in designs because of their highest shear to strength and stiffness to weight ratios. PVC foams were developed in the same years but they were firstly used commercially after 15 years.

Theoretical analysis of sandwich constructions started after the World War II. Two main textbooks written firstly about sandwich construction were published in 1960s by Plantema and Allen [3]. In 1990s Dan Zenkert published a third classic textbook [4] in this area and he summarized all studies on sandwich construction.

Dynamic response of structures under crash loads have been investigating since the second half of 20^{th} century. The purpose of this discipline is increasing the crashworthiness of engineering structures and occupant safety. National Advisory Committee for Aeronautics (NACA) and Federal Aviation Administration (FAA) has performed a series of crash tests of transport aircrafts. NACA has focused on energy absorbing components of structure. US Army sponsored the development of crash codes for modeling dynamic response of airframe structures with lumped-masses, beams and nonlinear springs. Many experimental studies were performed on

crashworthy concept and were applied real engineering structures such as aircraft fuselages, helicopter sub-floors, automobile chassis and frame structure, marine structures. A New generation of crash codes has been developed to accurately simulate the nonlinear, transient dynamic response of airframe structures. These finite elements codes, such as LS-DYNA3D, MSC.DYTRAN and PAM-CRASH use an explicit solver, which unlike an implicit code, does not need to repetitively decompose large global stiffness matrices. In 1997 Vehicle Technology Directorate researched on such kind of computer codes validating experimental data to efficiently investigate structural crash dynamics and crashworthy. As a part of that work a full-scale crash test of a Sikorsky helicopter was performed to generate experimental data for correlation of computer codes.

Fasanella and Jackson [5] have published a report on a full-scale crash test of a prototype composite helicopter performed at the Impact Dynamics Research Facility at NASA Langley Research Center in 1999. As crashworthiness criteria Military Standard MIL-STD-1290A was considered for design impact conditions and human safety requirements. Experimental data were correlated with numerical results taken from a explicit transient dynamic finite element code.

In order to examine failure modes and to model delamination growth, Dr. Fleming (Florida Institute of Technology) was studied on fracture based crash modeling by MSC.DYTRAN [6].

In Eurocopter Deutschland, for several years MSC.DYTRAN has been using to investigate the crashworthy behavior of composite fuselage and its components, [7]. CRASURV project has been carried out in the context of the Fourth Framework (BRITE-EURAM Programme funded by the European Union) to investigate the dynamic response and complex collapse mechanisms of composite frames. Vicente and Martinez [8] have investigated crashworthy behavior of sinusoidal shape longitudinal bulkheads in the sub-floor. Bisagni [9] has investigated the crash behavior and energy absorption capability of the sub-floor structural intersections by experimental drop tests and finite element analysis.

On the other hand through the HeliSafe project some researches have been performed to improve the survivability of occupants in helicopter crashes and to minimize the risk of injuries. Johnson and Lützenburger [10] from DLR (German Aerospace Center) have investigated helicopter cockpit crash safety using MADYMO.

In order to model failure of sandwich composites in impact loads many researches have been performed so far.

1.2 Scope of the study

The priority of this study is to maintain a preliminary sandwich structure for helicopter sub-floor to meet structural needs together with occupant safety in a crashing event with ground. Also with this study it is purposed to gain ability to model composite failure mechanisms numerically and examining them through the change of design of structural elements. The finally a vertical acceleration value on the pilot will present the reliability of structure designed.

This study is a preliminary for the detailed design study and optimization of the structure of the helicopter.

2. SANDWICH THEORIES

2.1 Sandwich Beam Theory

Beams as a structural component are considered to bear bending, tension and rarely torsion loads. Such beams constructed from isotropic-like materials have an advantage carrying transverse shear loads due to their high transverse modulus G. Lightweight sandwich beams generally have relatively soft cores and core material has very small transverse modulus. It is necessary to increase thickness of the cores to increase the shear rigidity. When a sandwich beam deflected under transverse loads, shear deflections occurs mainly in core materials. Because facing sheets generally high in plane elastic modulus, bending stresses carried mostly by them. Core material must be rigid enough to deflect simultaneously with facings. It can not be too rigid or too soft because of debonding failure limits and shear stress limits respectively. The Figure 2.1.1 shows estimated beam deflection behaviors under uniform transverse loading. The left figure is behavior of beam having high modulus core, and right figure models behavior of relatively low modulus core.

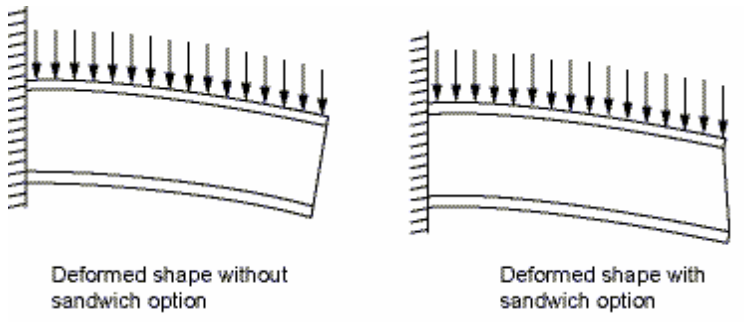

Figure 2.1 Transverse deflections without/with sandwich option
ANSYS Element Reference [11]

Sandwich option separate the reaction of beam into two categories for this simple loading as bending and shear reactions. Facing sheets are for bending and the core is for shear response of beam.

2.1.1 Flexural Rigidity and Bending Stresses

In order to calculate stress and strains through the height of an isotropic beam due to bending moment, just distance from the neutral axis and inertial moment of section is needed (of course moment load is known). But it is not enough for sandwich beam because of its heterogenic nature in cross-section. To solve this problem the flexural rigidity concept was developed. It helps us to calculate overall response of beam under the same bending moment. However; contributions of each separate section are calculated individually by using their modulus.

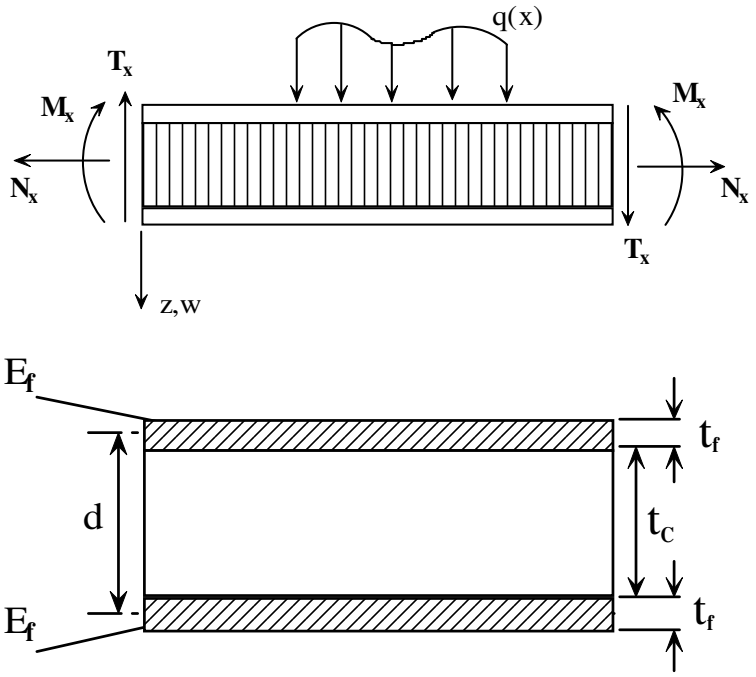

Figure 2.2 Sign convention for sandwich beams

The flexural rigidity D can be written for cross-section in Figure 2.2 as follow:

$$D = \int Ez^2 dz = \frac{E_f t_f^3}{6} + \frac{E_f t_f d^2}{2} + \frac{E_c t_c^3}{12} = 2D_f + D_0 + D_C \qquad [2.1]$$

Using strain definition for bended beams, bending stresses can be written in both face sheets and core. Stresses due to bending moment vary linearly across the thickness of each section. Resulting from this approach, maximum stresses occur in the free surfaces of face sheet materials. The moment direction assigns the tension and compression side of neutral axis. The face and core stresses are

$$\sigma_f = \frac{M_x z E_f}{D} \quad \text{for } \frac{t_c}{2} < |z| < \frac{t_c}{2} + t_f \qquad [2.2]$$

$$\sigma_c = \frac{M_x z E_c}{D} \quad \text{for } |z| < \frac{t_c}{2} \qquad [2.3]$$

There is a big jump in the stress distribution at core/face interface and stresses are discrete-linear when the face sheet plies stacked from different constituents.

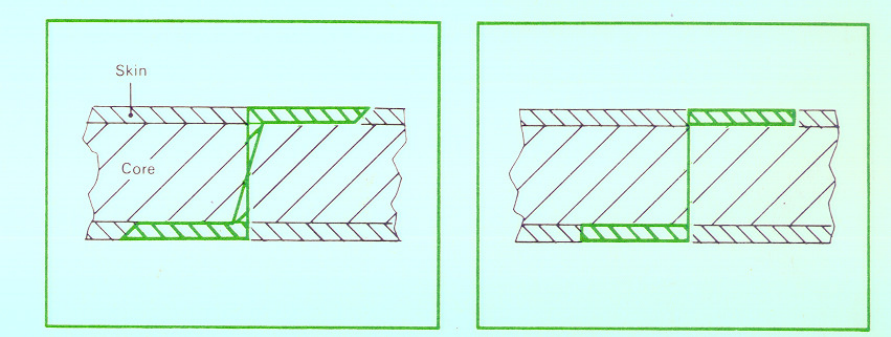

Figure 2.3 Bending stress distributions through the thickness of sandwich beam [12]

2.1.2 Shear Rigidity and Shear Stresses

The shear stiffness of a cross-section is defined by transverse force and shear strain as follow;

$$S = \frac{T_x}{\gamma} \qquad [2.4]$$

For a general cross-section shear stiffness can be predicted from energy balance of applied loads vs. the strain energy of the system. The shear stiffness, S, is computed by taking average value of shear angles through the thickness of beam. Using energy balance;

$$\frac{1}{2} T_x \gamma = \frac{1}{2} \int \tau_{xz}(z)\, \gamma_{xz}(z)\, dz \qquad [2.5]$$

Using some approximations for sandwich with thin faces, $t_f << t_c$, weak core, $E_c << E_f$, and shear modulus of face-sheets G_f large, it is seen that

$$\tau_{xz} = \frac{T_x}{d} \qquad [2.6]$$

then Equation [2.5] becomes

$$\frac{1}{2} T_x \gamma = \frac{1}{2} \int_{-t_c/2}^{t_c/2} \frac{T_x}{d} \frac{T_x}{G_c d} dz = \frac{T_x^2 t_c}{2 G_c d^2} \qquad [2.7]$$

yields that shear stiffness for general cross-section;

$$S = \frac{G_c d^2}{t_c} \qquad [2.8]$$

Considering a unit section of beam in Figure 2.2 with dx width, equilibrium equation can be written as;

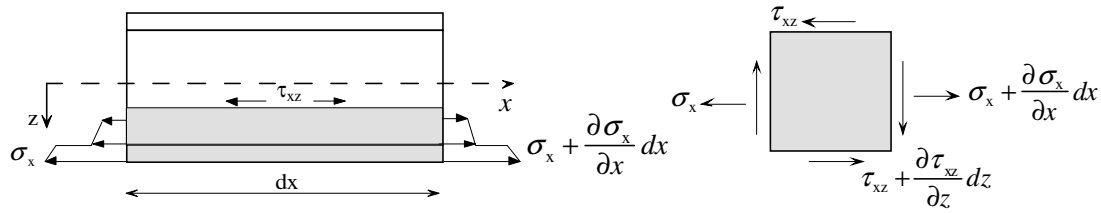

Figure 2.4 Equilibrium state in beam section with *dx* width

$$\frac{d\sigma_x}{dx}+\frac{d\tau_{xz}}{dz}=0 \quad \rightarrow \quad \tau_{xz}(z)=\int_z^{(d+t_f)/2}\frac{d\sigma_x}{dx}dz \qquad [2.9]$$

Distortional stresses are zero on free surfaces (at $d/2 + t_f$). Using the relation below;

$$\frac{dM_x}{dx}=T_x \qquad [2.10]$$

where T is transverse force, we get;

$$\tau=\frac{T_x}{D}\int_z^{(d+t_f)/2}Ezdz=\frac{T_xB(z)}{D} \qquad [2.11]$$

B(z) is the first moment of area and calculated for core material where $|z|<t_c/2$ as;

$$B(z)=\frac{E_f t_f d}{2}+\frac{E_c}{2}\left(\frac{t_c}{2}-z\right)\left(\frac{t_c}{2}+z\right) \qquad [2.12]$$

introducing the Equation [2.6] leads;

$$\tau_c(z)=\frac{T_x}{D}\left[\frac{E_f t_f d}{2}+\frac{E_c}{2}\left(\frac{t_c^2}{4}-z^2\right)\right] \qquad [2.13]$$

and similarly for skin materials where $t_c/2 \le |z| \le t_c/2 + t_f$

$$B(z)=\frac{E_f}{2}\left(\frac{t_c}{2}+t_f-z\right)\left(\frac{t_c}{2}+t_f+z\right) \qquad [2.14]$$

$$\tau_f(z) = \frac{T_x}{D}\frac{E_f}{2}\left(\frac{t_c^2}{4} + t_c t_f + t_f^2 - z^2\right) \qquad [2.15]$$

The maximum shear stress is predicted in the neutral axis of beam (z = 0) and distribution of shear stress through the thickness of sandwich beam as Figure 2.5;

$$\tau_{c,max}(z=0) = \frac{T_x}{D}\left(\frac{E_f t_f d}{2} + \frac{E_c t_c^2}{8}\right) \qquad [2.16]$$

In the core/face interface;

$$\tau_{c,min} = \tau_{f,max} = \tau\left(\frac{t_c}{2}\right) = \frac{T_x}{D}\left(\frac{E_f t_f d}{2}\right) \qquad [2.17]$$

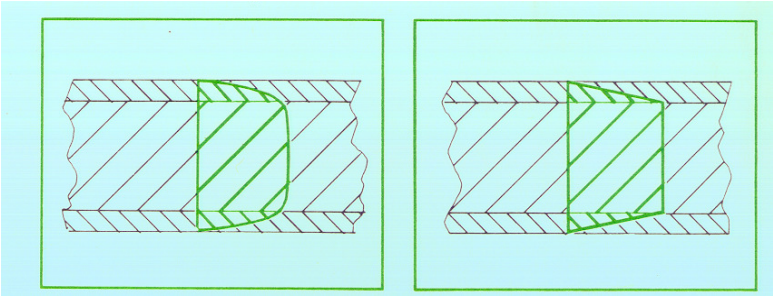

Figure 2.5 Shear stress distributions through the thickness of sandwich beam [12]

2.1.3 Approximations in Stress Calculations

Assuming weak core $E_c << E_f$, the stresses can be written

$$\sigma_c(z) = 0, \qquad \sigma_f(z) = \frac{MzE_f}{(D_0 + 2D_f)} \qquad [2.18]$$

$$\tau_c(z) = \frac{E_f t_f d}{2(D_0 + 2D_f)} \quad , \quad \tau_f(z) = \frac{Q}{D_0 + 2D_f}\frac{E_f}{2}\left(\frac{t_c^2}{4} + t_c t_f + t_f^2 - z^2\right) \qquad [2.19]$$

When the core is weak, $E_c << E_f$, and the faces are thin, $t_f << t_c$, then the formula reduces to the simplest possible form

$$\sigma_c(z) = 0, \quad \sigma_f(z) = \pm\frac{M}{t_f d}, \quad \tau_c(z) = \frac{Q}{d}, \text{ and } \tau_f(z) = 0 \qquad [2.20]$$

This simplifies the principal load carrying and stress distribution in a sandwich construction to the faces carry bending moments as tensile and compressive stresses and the core carries transverse forces as shear stresses, represented in Figure [2.6];

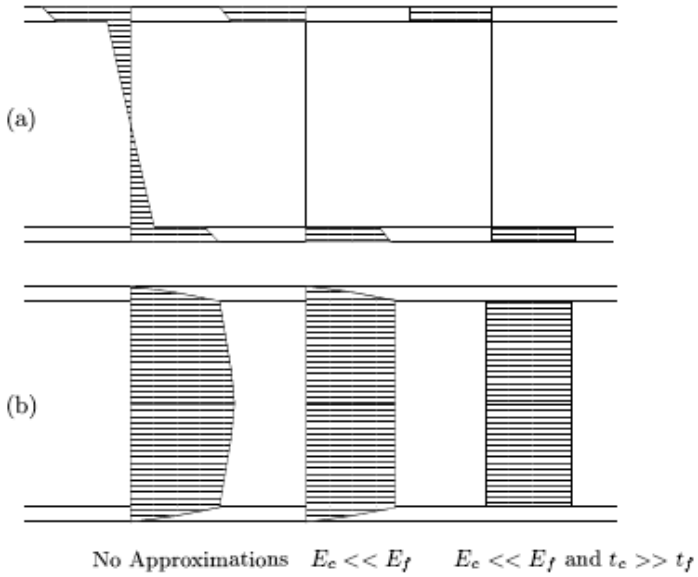

Figure 2.6 Direct (a) and shear (b) stresses with some approximations [4]

2.1.4 Analytical Solutions to Sandwich Beams

In classical plate theory shear deformations are neglected compared to the bending deflection. But for short beams with low stiffness this deformation must be included. This is usually called as Timoshenko beam theory [13]. The deformation consist of two parts

(i) deformation due to bending moments > w_b

(ii) deformation due to transverse forces > w_s

For a sandwich with this faces the two deformation parts may be superimposed as in Figure [2.7],

$$w = w_b + w_s \qquad [2.21]$$

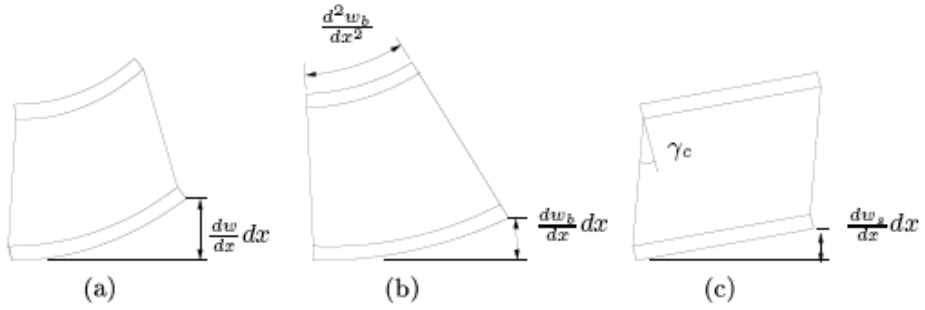

Figure 2.7 Total, bending and shear deformation [4]

Both "Classical" and "Timoshenko" models rest on the assumptions of small deformations and linear elastic isotropic material behavior. First order shear deformation theory assumes cross sections remain plane and rotate about the neutral axis but do not remain normal to the deformed longitudinal axis. The deviation from normality is produced by a transverse shear that is assumed to be constant over the cross section. The kinematic assumptions for the in-plane and out-of-plane deformations can be written as

$$u(z) = u_0 + z\psi_x \text{ and } w = w_b + w_s \qquad [2.22]$$

where the in-plane deformation u is thus linear function in z, and ψ_x is the cross section rotation which only depends on the bending deformation w_b of the beam.

$$\psi_x = -\frac{dw_b}{dx} \qquad [2.23]$$

Constitutive equation;

$$\sigma_x = E\varepsilon_x \qquad [2.24]$$

The faces of sandwich panels are thin enough to behave like membranes when shear deformation is studied. Thus any transverse shear deformation may take place without being resisted by any bending of the faces about their individual neutral axes. This is equivalent to the concept of partial deflections; bending causes in-plane stresses and transverse forces causes shear stresses and deformations. This study only considers stresses and strains arising from the bending moment and transverse forces of the beam.

Using the assumptions in Equation [2.20] the in-plane normal stress is obtained as

$$\sigma_f = -E_f z \frac{\partial^2 w_b}{\partial x^2} \qquad [2.25]$$

and the transverse shear stress

$$\tau_c(z) = \frac{Q}{d} \qquad [2.26]$$

Considering cross-section on a sandwich beam in Figure [2.4], summing the individual cross sectional moments with respect to neutral axis, we obtain the resultant moment for whole cross section.

$$M = \int\int z\sigma_x dz dy \qquad [2.27]$$

The sum of all shear stresses on the cross section is the definition of the shear resultant Q.

$$Q = \int\int \tau_{xz} dz dy \qquad [2.28]$$

The sum of all direct stresses on the cross section does not play a role in linear beam theory since it does not contribute to the deflection *w*.

Considering unit beam length the in-plane force in the upper and lower face can be written,

$$N_1 = -\int_{-t_f/2}^{t_f/2} \left[E_f (z - d/2) \frac{\partial^2 w_b}{\partial x^2} \right] dz = \frac{E_f t_f d}{2} \frac{\partial^2 w_b}{\partial x^2} = \frac{D_0}{d} \frac{\partial^2 w_b}{\partial x^2}$$

$$N_2 = -\int_{-t_f/2}^{t_f/2} \left[E_f (z + d/2) \frac{\partial^2 w_b}{\partial x^2} \right] dz = -\frac{E_f t_f d}{2} \frac{\partial^2 w_b}{\partial x^2} = -\frac{D_0}{d} \frac{\partial^2 w_b}{\partial x^2}$$

and the moment due to the in-plane forces becomes

$$M_0 = N_1(-\frac{d}{2}) + (-N_2)\frac{d}{2} = -D_0 \frac{\partial^2 w_b}{\partial x^2} \qquad [2.29]$$

The resultant moment in the core is

$$M_c = -\int_{-(d-t_f)/2}^{(d-t_f)/2} \left[E_c(z) \frac{\partial^2 w_b}{\partial x^2} \right] dz = -\frac{E_c t_c^3}{12} \frac{\partial^2 w_b}{\partial x^2} = -D_c \frac{\partial^2 w_b}{\partial x^2} \qquad [2.30]$$

and the faces

$$M_f = -\int_{-t_f/2}^{t_f/2} \left[E_f z (z - d/2) \frac{\partial^2 w_b}{\partial x^2} \right] dz = -\frac{E_f t_f^3}{12} \frac{\partial^2 w_b}{\partial x^2} = -D_f \frac{\partial^2 w_b}{\partial x^2} \qquad [2.31]$$

Total bending moment is

$$M = -(D_0 + D_f + D_c) \frac{\partial^2 w_b}{\partial x^2} = -D \frac{\partial^2 w_b}{\partial x^2} \qquad [2.32]$$

The response of sandwich beam is defined by two terms; flexural rigidity D and shear stiffness S,

$$D = -\frac{M}{d^2 w_b / dx^2} \text{ and } S = \frac{Q}{dw_s / dx} \quad [2.33]$$

Using [2.21], the contribution to the curvature becomes

$$\frac{\partial^2 w_b}{\partial x^2} = -\frac{M}{D} + \frac{1}{S}\frac{dQ}{dx} \quad [2.34]$$

From equilibrium of bending moments in Figure [2.8], it is found that $dM / dx = Q$, and by using the definitions of Equation [2.33] we find a relation between the partial deflections as

$$\frac{dw_s}{\mathrm{dx}} = -\frac{D}{S}\frac{\partial^3 w_b}{\partial x^3} \quad [2.35]$$

from the vertical equilibrium;

$$q + \frac{dQ}{dx} + N\frac{\partial^2 w}{\partial x^2} = 0 \quad [2.36]$$

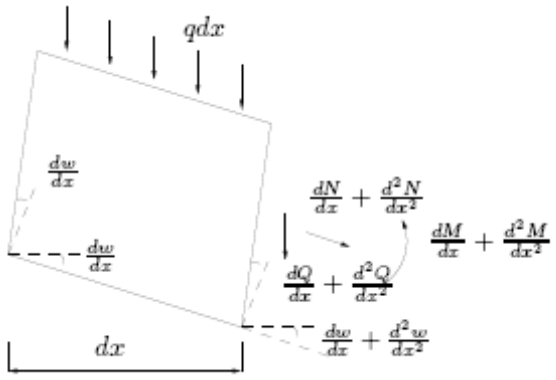

Figure 2.8 Distorted beam element [4]

Rewriting [2.36] gives;

$$S\frac{\partial^2 w_s}{\partial x^2} + N\frac{\partial^2 w}{\partial x^2} = -q \quad [2.37]$$

In the case of pure bending or small deformations when N is zero, an equation in w_s only is obtained. Rewriting Eq. [2.37] using Eq. [2.35] gives the governing equation in w_b

$$D + \frac{\partial^4 w_b}{\partial x^4} - N\frac{\partial^2 w}{\partial x^2} = q \qquad [2.38]$$

Rewriting this equation using the relation between w_s and w_b the governing equation can be written without the use of partial deflection as

$$D\frac{\partial^4 w}{\partial x^4} = \left(1 - \frac{D_0}{S}\right)\left(q + N\frac{\partial^2 w}{\partial x^2}\right) \qquad [2.39]$$

2.2 Sandwich Plate Theory

In the following section, analytical solutions to plate bending will be introduced. The theory is based on small deformation plate bending analysis by Timoshenko and Woinowsky-Krieger [13] which is extended to account for transverse shear deformation following the work by Libove and Batdorf. It is assumed that transverse normal stiffness of the core is infinite and thus keeping the distance between the centroids of the faces (d) constant. The theory is developed for orthotropic plates with x- and y-axis being the principal axes of orthotropy. This means that the properties of the plate are fully described by seven constants, the flexural rigidities D_x and D_y, twisting stiffness D_{xy}, the Poisson's ratios ν_{yx} and ν_{xy}, and the shear rigidities S_x and S_y.

The coordinate system and positive directions are defined in Figure [2.9]. It is assumed that the shear strain is constant over the cross section (thin-face approximation) so the in-plane deformations for the classic Reissner/Mindlin kinematics can be used. These are

$$\begin{aligned} u &= u_0 + z\theta_x, \\ v &= v_0 + z\theta_y, \\ w &= w_0 \end{aligned} \qquad [2.40]$$

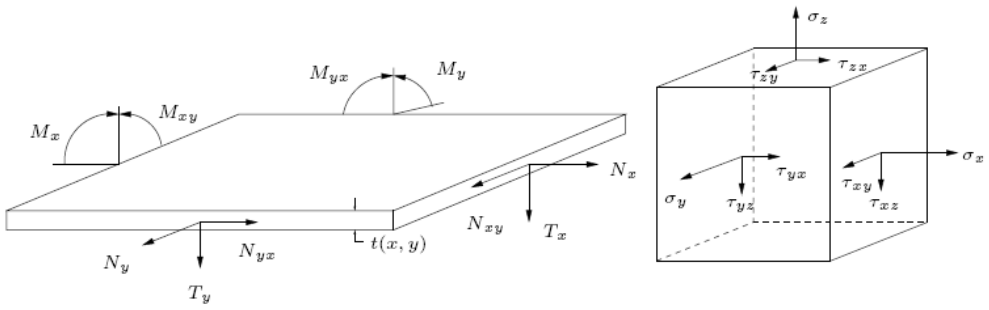

Figure 2.9 Sign convention for plate analysis [4]

Assuming strains to be much smaller than unity, the strain-displacement relations are defined as;

$$\varepsilon_x = \frac{\partial u}{\partial x} = \varepsilon_{x0} + z_x \frac{\partial \theta_x}{\partial x}$$
$$\varepsilon_y = \frac{\partial v}{\partial y} = \varepsilon_{y0} + z_y \frac{\partial \theta_y}{\partial y} \qquad [2.41]$$
$$\gamma_{xy} = \frac{\partial u}{\partial y} + \frac{\partial v}{\partial x} = \gamma_{xy0} + z_x \frac{\partial \theta_x}{\partial y} + z_y \frac{\partial \theta_y}{\partial x}$$

The bending moments and transverse forces can be written as functions of the displacement field *w*. The curvatures of the plate can be written as,

$$\kappa_x = -\frac{\partial^2 w}{\partial x^2}, \quad \kappa_y = -\frac{\partial^2 w}{\partial y^2}, \text{ and } \kappa_{xy} = -\frac{\partial^2 w}{\partial x \partial y} \qquad [2.42]$$

The component κ_{xy} is a twisting curvature, stating how the x-direction mid-plane slope changes with y. The Poisson's ratios;

$$\nu_{xy} = -\frac{\partial^2 w / \partial y^2}{\partial^2 w / \partial x^2} \text{ and } \nu_{yx} = -\frac{\partial^2 w / \partial x^2}{\partial^2 w / \partial y^2} \qquad [2.43]$$

Assuming that only a single load is allowed to act on the plate at a time, the plate equations can be derived by collecting the contributions from each load. This leads to the following equations for the curvatures

$$\frac{\partial^2 w}{\partial x^2} = -\frac{M_y}{D_x} + \nu_{yx} \frac{M_y}{D_y} + \frac{1}{S_x} \frac{\partial Q_x}{\partial x} \qquad [2.44]$$

$$\frac{\partial^2 w}{\partial y^2} = -\frac{M_x}{D_y} + \nu_{xy} \frac{M_x}{D_x} + \frac{1}{S_y} \frac{\partial Q_y}{\partial y} \qquad [2.45]$$

$$\frac{\partial^2 w}{\partial x \partial y} = -\frac{M_{xy}}{D_{xy}} + \frac{1}{2S_x} \frac{\partial Q_x}{\partial y} + \frac{1}{2S_y} \frac{\partial Q_y}{\partial x} \qquad [2.46]$$

Equilibrium equations are defined by studying Figure [2.10], assuming an increment change in all forces and bending moments over the differential element. By projecting all forces onto the z-axis -see Figure [2.11]-, the vertical equilibrium is found. For the normal force N_x;

$$-N_x \frac{\partial w}{\partial x} dy + (N_x + \frac{\partial N_x}{\partial x} dx) dy (\frac{\partial w}{\partial x} + \frac{\partial^2 w}{\partial x^2} dx) \quad [2.47]$$

and the projection of the shear force N_{xy} is similarly

$$-N_{xy} \frac{\partial w}{\partial x} dx + (N_{yx} + \frac{\partial N_{yx}}{\partial y} dy) dx (\frac{\partial w}{\partial x} + \frac{\partial^2 w}{\partial x \partial y} dx) \quad [2.48]$$

By including the rest of the terms and omitting higher order terms in dx and dy one arrives at

$$\frac{\partial Q_x}{\partial x} + \frac{\partial Q_y}{\partial y} + q + N_x \frac{\partial^2 w}{\partial x^2} + N_y \frac{\partial^2 w}{\partial y^2} + N_{xy} \frac{\partial^2 w}{\partial x \partial y} + N_{yx} \frac{\partial^2 w}{\partial x \partial y} = 0 \quad [2.49]$$

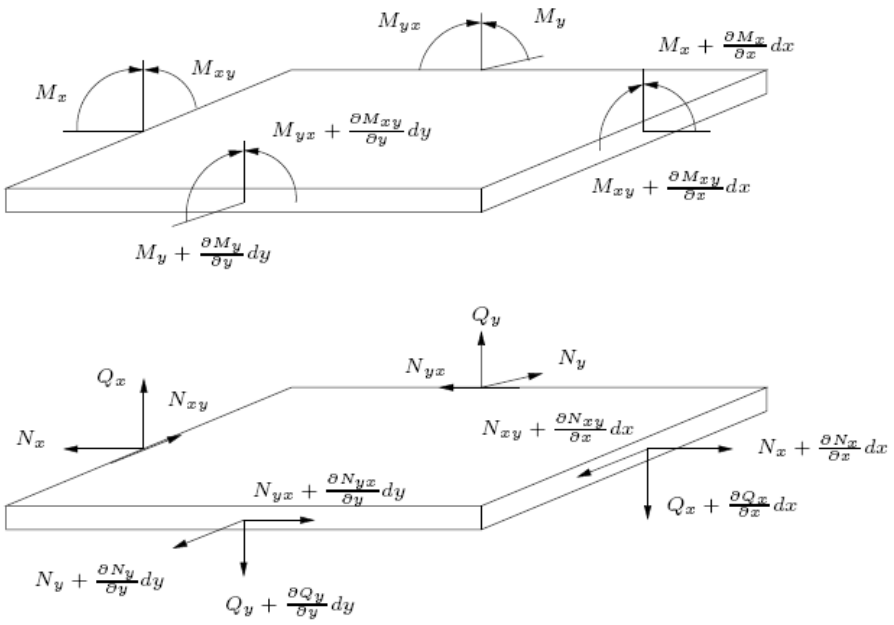

Figure 2.10 Bending moments and forces acting on differential element [4]

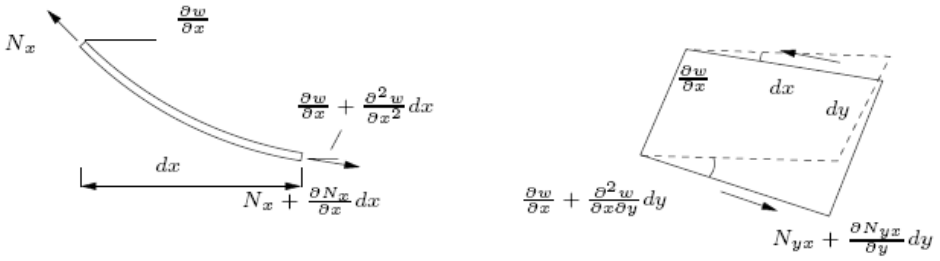

Figure 2.11 Force projections [4]

From equilibrium of the bending moments about the x-, y- and z-axes the following equations are obtained

$$Q_{\mathrm{x}} - \frac{\partial M_{\mathrm{x}}}{\partial x} - \frac{\partial M_{\mathrm{yx}}}{\partial y} = 0 \qquad [2.50]$$

$$Q_{\mathrm{y}} - \frac{\partial M_{\mathrm{y}}}{\partial y} - \frac{\partial M_{\mathrm{xy}}}{\partial x} = 0 \qquad [2.51]$$

$$N_{\mathrm{xy}} = N_{\mathrm{yx}} \qquad [2.52]$$

Here $M_{\mathrm{yx}} = M_{\mathrm{xy}}$ since $\tau_{\mathrm{xy}} = \tau_{\mathrm{yx}}$. By assuming that the normal forces N are constant throughout the plate and that they do not change as the plate bends the analysis is restricted to small deformations. Inverting the relations above the following expression for the bending moments arise

$$M_{\mathrm{x}} = -\frac{D_{\mathrm{x}}}{(1-\nu_{\mathrm{xy}}\nu_{\mathrm{yx}})}\left[\frac{\partial}{\partial x}\left(\frac{\partial w}{\partial x} - \frac{Q_{\mathrm{x}}}{S_{\mathrm{x}}}\right) + \nu_{\mathrm{yx}}\frac{\partial}{\partial y}\left(\frac{\partial w}{\partial y} - \frac{Q_{\mathrm{y}}}{S_{\mathrm{y}}}\right)\right] \qquad [2.53]$$

$$M_{\mathrm{y}} = -\frac{D_{\mathrm{y}}}{(1-\nu_{\mathrm{xy}}\nu_{\mathrm{yx}})}\left[\frac{\partial}{\partial y}\left(\frac{\partial w}{\partial y} - \frac{Q_{\mathrm{y}}}{S_{\mathrm{y}}}\right) + \nu_{\mathrm{xy}}\frac{\partial}{\partial x}\left(\frac{\partial w}{\partial x} - \frac{Q_{\mathrm{x}}}{S_{\mathrm{x}}}\right)\right] \qquad [2.54]$$

$$M_{\mathrm{xy}} = -\frac{D_{\mathrm{xy}}}{2}\left[\frac{\partial}{\partial x}\left(\frac{\partial w}{\partial y} - \frac{Q_{\mathrm{y}}}{S_{\mathrm{y}}}\right) + \frac{\partial}{\partial y}\left(\frac{\partial w}{\partial x} - \frac{Q_{\mathrm{x}}}{S_{\mathrm{x}}}\right)\right] \qquad [2.55]$$

By arranging Equation [2.49], rewriting these equations to obtain equations in one single variable;

$$\frac{\partial^2 M_x}{\partial x^2} + 2\frac{\partial^2 M_{xy}}{\partial x \partial y} + \frac{\partial^2 M_y}{\partial y^2} = \frac{\partial Q_x}{\partial x} + \frac{\partial Q_y}{\partial y} = -\bar{q} \qquad [2.56]$$

with

$$\bar{q} = q + N_x \frac{\partial^2 w}{\partial x^2} + 2N_{xy} \frac{\partial^2 w}{\partial x \partial y} + N_y \frac{\partial^2 w}{\partial y^2} \qquad [2.57]$$

Partial deflections due to bending and shear are introduced by assuming only one mode of deformations at a time, and the displacement fields due to bending w_b, and transverse shear w_s can be separated. The total deflection is then found by superimposing these contributions. Introducing specific relations between the transverse forces and the shear part of the deformations as

$$w = w_b + w_s, \quad Q_x = S_x \frac{\partial w_s}{\partial x} \text{ and } Q_y = S_y \frac{\partial w_s}{\partial y} \qquad [2.58]$$

Assuming that $z_x = z_y = z$ are measured from the geometric middle plane of the plate, the following approximate set of cross-section rotations are written;

$$\theta_x = -\frac{\partial w_b}{\partial x} \text{ and } \theta_y = -\frac{\partial w_b}{\partial y} \qquad [2.59]$$

by letting $u_0 = v_0 = 0$ yields

$$\begin{aligned} &u = -z\frac{\partial w_b}{\partial x}, v = -z\frac{\partial w_b}{\partial y} \\ &\varepsilon_x = -z\frac{\partial^2 w_b}{\partial x^2}, \quad \varepsilon_y = -z\frac{\partial^2 w_b}{\partial y^2}, \quad \gamma_{xy} = -2z\frac{\partial^2 w_b}{\partial x \partial y} \end{aligned} \qquad [2.60]$$

Equations [2.53], [2.54] and [2.55] can now be transformed to

$$M_x = -\frac{D_x}{(1-\nu_{xy}\nu_{yx})}\left[\frac{\partial^2 w_b}{\partial x^2}+\nu_{yx}\frac{\partial^2 w_b}{\partial y^2}\right]$$
$$M_y = -\frac{D_y}{(1-\nu_{xy}\nu_{yx})}\left[\frac{\partial^2 w_b}{\partial y^2}+\nu_{xy}\frac{\partial^2 w_b}{\partial x^2}\right] \qquad [2.61]$$
$$M_{xy} = -D_{xy}\frac{\partial^2 w_b}{\partial x \partial y}$$

It is seen that the partial deflection w_b represents the classical plate bending deformation. Since the shear deflection does not rotate the cross-section, all bending moments depend on bending deflection (w_b). The relation between partial deflections can be found substituting the above equations into [2.50] and [2.51],

$$S_x\frac{\partial w_s}{\partial x} = -\frac{D_x}{(1-\nu_{xy}\nu_{yx})}\left[\frac{\partial^3 w_b}{\partial x^3}+\nu_{yx}\frac{\partial^3 w_b}{\partial x \partial y^2}\right]-D_{xy}\frac{\partial^3 w_b}{\partial x \partial y^2} \qquad [2.62]$$

$$S_y\frac{\partial w_s}{\partial y} = -\frac{D_y}{(1-\nu_{xy}\nu_{yx})}\left[\frac{\partial^3 w_b}{\partial y^3}+\nu_{yx}\frac{\partial^3 w_b}{\partial x^2 \partial y}\right]-D_{xy}\frac{\partial^3 w_b}{\partial x^2 \partial y} \qquad [2.63]$$

By differentiating the above equation, using Eq. [2.60] and inserting into the equilibrium equation [2.56],

$$S_x\frac{\partial^2 w_s}{\partial x^2}+S_y\frac{\partial^2 w_s}{\partial y^2} = -\bar{q} \qquad [2.64]$$

Using [2.62] and [2.63] the equilibrium equation above may be expressed by

$$\frac{D_x}{(1-\nu_{xy}\nu_{yx})}\frac{\partial^4 w_b}{\partial x^4}+\left[\frac{\nu_{yx}D_x+\nu_{xy}D_y}{(1-\nu_{xy}\nu_{yx})}+2D_{xy}\right]\frac{\partial^4 w_b}{\partial x^2 \partial y^2}+\frac{D_y}{(1-\nu_{xy}\nu_{yx})}\frac{\partial^4 w_b}{\partial y^4} = \bar{q} \qquad [2.65]$$

which is the differential equation in pure bending of an ordinary orthotropic plate. If we accept the concept of partial deflections, we can assume Eq. [2.64] to be valid for the case when the bending stiffness goes to infinity. Then all components in $\bar{q}$ takes the value of w_s so that Eq. [2.64] is in the terms of w_s. Similarly, Eq. [2.65] can be solved with respect to w_b by setting the deflection components on the right hand side equal to w_b. The two solutions do not depend on each other and the total solution can be obtained by superposition.

2.3 Two Dimensional FEA of Sandwich Plates

The displacement field expressed considering first order deformation theory as follow [15-19]

$$\begin{aligned} u(x, y, z, t) &= u_0(x, y, t) + z\psi_x(x, y, t) \\ v(x, y, z, t) &= v_0(x, y, t) + z\psi_y(x, y, t) \\ w(x, y, z, t) &= w_0(x, y, t) \end{aligned} \qquad [2.66]$$

where u, v, and w are the displacement components in the x, y, and z directions respectively; u_0 ,v_0 , and w_0 are the displacements of a point on the mid-plane (x, y, 0); ψ_x and ψ_y are the rotations of the cross-sections perpendicular to the x and y axes respectively.

Strain components based on the infinitesimal deformation can be expressed in linear form as follow;

$$\begin{aligned} \varepsilon_{xx} &= \varepsilon^o_{xx} + z\kappa^o_{xx} \\ \varepsilon_{yy} &= \varepsilon^o_{yy} + z\kappa^o_{xx} \\ \varepsilon_{zz} &= 0 \\ \varepsilon_{yz} &= \varepsilon^o_{yz} \\ \varepsilon_{xz} &= \varepsilon^o_{xz} \\ \varepsilon_{xy} &= \varepsilon^o_{xy} + z\kappa^o_{xy} \end{aligned} \qquad [2.67]$$

where

$$\begin{aligned} \varepsilon^o &= (\varepsilon^o_{xx}, \varepsilon^o_{yy}, \varepsilon^o_{xy})^{\mathrm{T}} = \left(\frac{\partial u_o}{\partial x}, \frac{\partial v_o}{\partial y}, \frac{\partial u_o}{\partial y} + \frac{\partial v_o}{\partial x} \right)^{\mathrm{T}} \\ \kappa^o &= (\kappa^o_{xx}, \kappa^o_{yy}, \kappa^o_{xy})^{\mathrm{T}} = \left(\frac{\partial \psi_x}{\partial x}, \frac{\partial \psi_y}{\partial y}, \frac{\partial \psi_x}{\partial y} + \frac{\partial \psi_y}{\partial x} \right)^{\mathrm{T}} \\ \varepsilon^s &= (\varepsilon^o_{xz}, \varepsilon^o_{yz}) = \left(\frac{\partial w_o}{\partial x} + \psi_x, \frac{\partial w_o}{\partial y} + \psi_y \right)^{\mathrm{T}} \end{aligned} \qquad [2.68]$$

The transverse shear strains are constant through the thickness of laminate in equations [2.67] and [2.68], so there is need for the shear correction factors.

The stress-strain relations of a lamina with respect to the three axes are given by

$$\begin{Bmatrix} \sigma_{xx} \\ \sigma_{yy} \\ \sigma_{xy} \end{Bmatrix} = \begin{bmatrix} Q_{11} & Q_{12} & Q_{16} \\ Q_{12} & Q_{22} & Q_{26} \\ Q_{16} & Q_{26} & Q_{66} \end{bmatrix} \begin{Bmatrix} \varepsilon_{xx} \\ \varepsilon_{yy} \\ \varepsilon_{xy} \end{Bmatrix} \quad [2.69]$$

$$\begin{Bmatrix} \sigma_{xz} \\ \sigma_{yz} \end{Bmatrix} = \begin{bmatrix} Q_{55} & Q_{54} \\ Q_{54} & Q_{44} \end{bmatrix} \begin{Bmatrix} \varepsilon_{xz} \\ \varepsilon_{yz} \end{Bmatrix} \quad [2.70]$$

where Q_{ij} are transformed material constants. The components of Q_{ij}'s are given as

$$[\mathbf{Q_{ij}}] = [\mathbf{T_1}]^{-1}[\bar{\mathbf{Q}}_{\mathbf{ij}}]_k[\mathbf{T_1}]^{-T} \quad (i, j = 1,2,6) \quad [2.71]$$

$$[\mathbf{Q_{ij}}] = [\mathbf{T_2}]^{-1}[\bar{\mathbf{Q}}_{\mathbf{ij}}]_k[\mathbf{T_2}]^{-T} \quad (i, j = 5,4) \quad [2.72]$$

in which T_1 and T_2 are the transformation matrices. $\bar{Q}_{ij}$'s are plane stress reduced elastic constants in the material axes of the k_{th} lamina.

$$[\mathbf{T_1}] = \begin{bmatrix} \cos^2\theta & \sin^2\theta & 2\cos\theta\sin\theta \\ \sin^2\theta & \cos^2\theta & -2\cos\theta\sin\theta \\ -\cos\theta\sin\theta & \cos\theta\sin\theta & \cos^2\theta - \sin^2\theta \end{bmatrix}$$

$$[\mathbf{T_2}] = \begin{bmatrix} \cos\theta & \sin\theta \\ -\sin\theta & \cos\theta \end{bmatrix}$$

$$[\bar{\mathbf{Q}}_{\mathbf{ij}}]_k = \begin{bmatrix} \bar{Q}_{11} & \bar{Q}_{12} & 0 \\ \bar{Q}_{12} & \bar{Q}_{22} & 0 \\ 0 & 0 & \bar{Q}_{66} \end{bmatrix} \quad (i, j = 1,2,6)$$

$$[\bar{\mathbf{Q}}_{\mathbf{ij}}]_k = \begin{bmatrix} \bar{Q}_{55} & 0 \\ 0 & \bar{Q}_{44} \end{bmatrix} \quad (i, j = 5,4) \quad [2.73]$$

where

$$\bar{Q}_{11} = \frac{E_x}{(1-\nu_{xy}\nu_{yx})}, \ \bar{Q}_{12} = \frac{\nu_{xy}E_y}{(1-\nu_{xy}\nu_{yx})}, \ \bar{Q}_{22} = \frac{E_y}{(1-\nu_{xy}\nu_{yx})},$$

$\bar{Q}_{66} = G_{xy}$, $\bar{Q}_{55} = G_{xz}$, $\bar{Q}_{44} = G_{yz}$, θ is the lamination angle.

Hamilton principle is used to derive the equations of motion appropriate for displacement field in Equation [2.69] to [2.73]. The principle can be stated in an analytical form as

$$\int_0^t \int_V (\sigma_{xx}\delta\varepsilon_{xx}+\sigma_{yy}\delta\varepsilon_{yy}+\sigma_{xy}\delta\varepsilon_{xy}+\sigma_{xz}\delta\varepsilon_{xz}+\sigma_{yz}\delta\varepsilon_{yz})dVdt+\int_0^t \int_A q\delta w_0 dxdydt$$
$$=\int_0^t \int_V \rho(\ddot{u}\delta u+\ddot{v}\delta v+\ddot{w}\delta w)dVdt \qquad [2.74]$$

Where V is the volume, A is the cross sectional area, ρ (x,y,z) is the density of the plate, q is the transverse load applied at the top surface of the plate and t is the time. Using equations from [2.66] to [2.73] in Eq. [2.74], integrating the resulting expression by parts and collecting the coefficients of δu_0, δv_0, δw_0, $\delta\psi_x$ and $\delta\psi_y$, the following equations

$$\delta u_0 : \frac{\partial N_{xx}}{\partial x}+\frac{\partial N_{xy}}{\partial y}=I_1\ddot{u}_0+I_2\ddot{\psi}_x$$

$$\delta v_0 : \frac{\partial N_{xy}}{\partial x}+\frac{\partial N_{yy}}{\partial y}=I_1\ddot{v}_0+I_2\ddot{\psi}_y$$

$$\delta w_0 : \frac{\partial Q_{xx}}{\partial x}+\frac{\partial Q_{yy}}{\partial y}+q=I_1\ddot{w}_0$$

$$\delta\psi_x : \frac{\partial M_{xx}}{\partial x}+\frac{\partial M_{xy}}{\partial y}-Q_{xx}=I_2\ddot{u}_0+I_3\ddot{\psi}_x$$

$$\delta\psi_y : \frac{\partial M_{xy}}{\partial x}+\frac{\partial M_{yy}}{\partial y}-Q_{yy}=I_2\ddot{v}_0+I_3\ddot{\psi}_y \qquad [2.75]$$

where the stress resultants $(N_{xx},N_{yy},N_{xy},M_{xx},M_{yy},M_{xy},Q_{xz},Q_{yz})$ and inertias (I_1,I_2,I_3) are given as

$$\begin{Bmatrix} N_{xx} & M_{xx} \\ N_{yy} & M_{yy} \\ N_{xy} & M_{xy} \end{Bmatrix} = \int_{\frac{-h}{2}}^{\frac{h}{2}} \begin{Bmatrix} \sigma_{xx} \\ \sigma_{yy} \\ \sigma_{xy} \end{Bmatrix} \begin{pmatrix} 1 & z \end{pmatrix} dz$$

$$\begin{Bmatrix} Q_{xz} \\ Q_{yz} \end{Bmatrix} = \int_{\frac{-h}{2}}^{\frac{h}{2}} \begin{Bmatrix} \sigma_{xz} \\ \sigma_{yz} \end{Bmatrix} dz$$

$$\begin{Bmatrix} I_1 \\ I_2 \\ I_3 \end{Bmatrix} = \int_{\frac{-h}{2}}^{\frac{h}{2}} \rho \begin{Bmatrix} 1 \\ z \\ z^2 \end{Bmatrix} dz \qquad [2.76]$$

The various stress resultants are given by

$$\begin{Bmatrix}\mathbf{N}\\ \mathbf{M}\end{Bmatrix}=\begin{bmatrix}\mathbf{A} & \mathbf{B}\\ \mathbf{B} & \mathbf{D}\end{bmatrix}\begin{Bmatrix}\varepsilon^0\\ \kappa^0\end{Bmatrix} \qquad \{\mathbf{Q}\}=\left[\mathbf{A}^{\mathbf{s}}\right]\{\varepsilon^{\mathrm{s}}\} \tag{2.77}$$

where $\mathbf{A_{ij}}, \mathbf{B_{ij}}, \mathbf{D_{ij}}$ and $\mathbf{A^s_{ij}}$ are the plate stiffnesses, defined by

$$\begin{aligned}(\mathbf{A_{ij}}, \mathbf{B_{ij}}, \mathbf{D_{ij}}) &= \int_{\frac{-h}{2}}^{\frac{h}{2}} \mathbf{Q_{ij}}(1, z, z^2)dz \qquad (i, j = 1,2,6)\\ (\mathbf{A^s}_{\mathbf{ij}}) &= \int_{\frac{-h}{2}}^{\frac{h}{2}} k_5^2 k_4^2 \mathbf{Q_{ij}} dz \qquad (i, j = 5,4)\end{aligned} \tag{2.78}$$

where k_5^2, k_4^2 are the shear correction factors. Using equations [2.75] to [2.78], the principle of virtual work equation can be expressed in the following form

$$\begin{aligned}&\int_0^t \int_A (\delta\varepsilon^{0\mathrm{T}}\mathbf{A}\varepsilon^0 + \delta\varepsilon^{0\mathrm{T}}\mathbf{B}\kappa^0 + \delta\kappa^{0\mathrm{T}}\mathbf{B}\varepsilon^0 + \delta\kappa^{0\mathrm{T}}\mathbf{D}\kappa^0 + \delta\varepsilon^{\mathrm{sT}}\mathbf{A}^{\mathrm{s}}\varepsilon^{\mathrm{s}})dAdt + \int_0^t \int_A qdwdAdt\\ &= \int_0^t \int_A \begin{bmatrix} I_1(\ddot{u}_0\delta u_0 + \ddot{v}_0\delta v_0 + \ddot{w}\delta w_0) + I_2(\ddot{\psi}_{\mathrm{x}}\delta u_0 + \ddot{\psi}_{\mathrm{y}}\delta v_0 + \ddot{u}_0\delta\psi_{\mathrm{x}} + \ddot{v}_0\delta\psi_{\mathrm{y}}) + \\ I_3(\ddot{\psi}_{\mathrm{x}}\delta\psi_{\mathrm{x}} + \ddot{\psi}_{\mathrm{y}}\delta\psi_{\mathrm{y}}) \end{bmatrix}\end{aligned} \tag{2.79}$$

The finite element equations are obtained by discretizing the plane region **R** into a number of isoparametric elements. Each element "e" has "n" nodes, where each node is identified with five degrees of freedom $U^{\mathrm{i}}_{(\mathrm{e})} = (u_0^{\mathrm{i}}, v_0^{\mathrm{i}}, w_0^{\mathrm{i}}, \psi_{\mathrm{x}}^{\mathrm{i}}, \psi_{\mathrm{y}}^{\mathrm{i}})_{(\mathrm{e})}$. For simplicity the same interpolation for all five variables can be assumed as,

$$u_0 = \sum_{\mathrm{i}=1}^{\mathrm{n}} N_{\mathrm{i}} u_0^{\mathrm{i}} \quad v_0 = \sum_{\mathrm{i}=1}^{\mathrm{n}} N_{\mathrm{i}} v_0^{\mathrm{i}} \quad w_0 = \sum_{\mathrm{i}=1}^{\mathrm{n}} N_{\mathrm{i}} w_0^{\mathrm{i}} \quad \psi_{\mathrm{x}} = \sum_{\mathrm{i}=1}^{\mathrm{n}} N_{\mathrm{i}} \psi_{\mathrm{x}}^{\mathrm{i}}$$

$$\psi_{\mathrm{y}} = \sum_{\mathrm{i}=1}^{\mathrm{n}} N_{\mathrm{i}} \psi_{\mathrm{y}}^{\mathrm{i}} \tag{2.80}$$

where $N_{\mathrm{i}}, i = 1, ..., n$, are the interpolation functions. The shape functions N_{i} for an element are functions of the two reference variables ξ and η (element coordinate system). If the generalized displacement vector $(U_{(\mathrm{e})} = [\mathbf{N}]^{(\mathrm{e})}\{\delta\}_{(\mathrm{e})})$ is known at all points within the element "e", the generalized mid-surface strains at any point given by Equation [2.67] can be expressed in terms of nodal displacements as follows:

$$\varepsilon^{0(\mathrm{e})} = [\mathbf{B}^0_{\varepsilon}]^{(\mathrm{e})}\{\delta\}_{(\mathrm{e})} \qquad \kappa^{0(\mathrm{e})} = [\mathbf{B}^0_{\kappa}]^{(\mathrm{e})}\{\delta\}_{(\mathrm{e})} \qquad \varepsilon^{\mathrm{s}(\mathrm{e})} = [\mathbf{B}^{\mathrm{s}}_{\varepsilon}]^{(\mathrm{e})}\{\delta\}_{(\mathrm{e})} \tag{2.81}$$

where $[\mathbf{B}_{\varepsilon}^{0}], [\mathbf{B}_{\kappa}^{0}]$ and $[\mathbf{B}_{\varepsilon}^{s}]$ are generated strain-displacement matrices. For arbitrary values of virtual displacements, Equation [2.79] finally leads to the following assembled equations

$$[\mathbf{M}]\{\ddot{\Delta}\} + [\mathbf{K}]\{\Delta\} = \{\mathrm{F}\} \qquad [2.82]$$

The unknown vector $\{\Delta\}$ is generated by the assemblage of element degrees of freedom $\{d\}_{\mathrm{e}}^{\mathrm{T}}, e = 1, ...$ (total degrees of freedom in the region **R**).

3. FAILURE THEORIES

Engineering composites have not so much deformation beyond elastic limit and structures are designed generally with a safety factor, i.e. for marine structures one third of elastic limit strength (σ_i^u). In fiber direction, tensile loadings have not major role in failure. But strength input values for failure criteria examined are taken in this direction. ASTM standard test methods for tensile properties of plastics (D 638-84) define tensile failure modes in the following terms and asymptotic shape as in figure below.

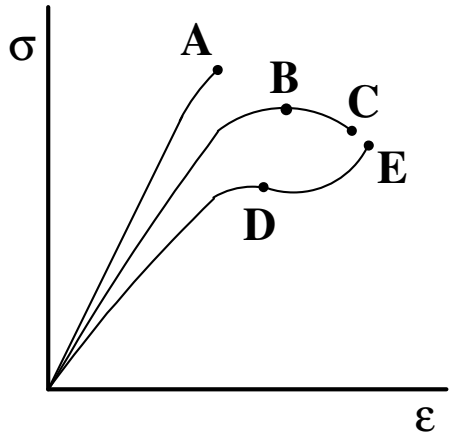

Figure 3.1 Tensile Failure Modes of Engineering Plastics

Defined by ASTM (24)

A & E tensile strength and elongation at break

B tensile strength and elongation at yield

C tensile stress and elongation at break

D tensile stress and elongation at yield

In local analysis of sandwich structural elements, there are some experienced failure modes. The following section gives information about global and local failure modes of honeycomb sandwich constructions [4, 14, 15, 20-26].

3.1 Local Strength Analysis of Sandwich Beams and Panels

3.1.1 Insufficient Strength Based Failures

3.1.1.1 Facing Failure

In sandwich panels and beams facing laminates are designed to meet allowable strength values under maximum tensile or compression stresses in direction considered. Ultimate strength values are determined from corresponding unidirectional testing of face-sheet material used in laminate. Allowable strength values are determined by designer. There must be enough safety margin under ultimate or failure strength of lamina in the direction considered. That safety factors may change according to material type, manufacturing methods and also structure to be designed. Maximum values of stresses are predicted from the upper and lower surfaces of beam or panel. For a safe design maximum values of stress without certain safety margin must be as follow:

$$\sigma_{fx} = \frac{M_x z E_{fx}}{D_x} \leq \sigma_{fx}^{u} \quad \text{and in the y direction } \sigma_{fy} = \frac{M_y z E_{fy}}{D_y} \leq \sigma_{fy}^{u} \qquad [3.1]$$

where z denotes the distance of middles of laminas from the neutral axis of laminate or sandwich.

On the other hand stress based examining of facings is insufficient method in failure analysis. Because even stresses are calculated under the ultimate or allowable limits deformations or strains may exceed the allowable deformation or strain limits. Therefore; it might be useful approach to consider design allowables as strain allowables too.

3.1.1.2 Transverse Shear Failure

In sandwich concept, the core materials are mainly subjected to shear and carry all transverse shear loads. Assuming weak core such that $E_c << E_f$ then in plane normal stresses will mostly carried by facings and only transverse shear stress components will exist on the core material. For a unit wide of beam, maximum design shear stresses without certain safety margin must be as follow:

$$\tau_{cxz} = \frac{T_x}{d} \le \tau^u{}_{cxz} \quad \text{and} \quad \tau_{cyz} = \frac{T_x}{d} \le \tau^u{}_{cyz} \qquad [3.2]$$

3.1.1.3 Flexural Core Crushing

Under bending action of a panel, core material must be rigid enough to prevent face sheets from moving each other. Maximum bending moments of sandwich shell elements are put in the following formula to calculate core crushing stress.

$$\sigma_{crush} = \frac{M_x^2}{d\ D_{zx}} + \frac{M_y^2}{d\ D_{zy}} \qquad [3.3]$$

where "d" is distance between mid-planes of face-sheets and "D_{zx}" and "D_{zy}" flexural stiffness values for panel strips parallel to the x and y directions respectively.

$$D_{zx} = \frac{d^2}{\left(\frac{1-\nu_{xy}\nu_{yx}}{E_x t}\right)_t + \left(\frac{1-\nu_{xy}\nu_{yx}}{E_x t}\right)_b}$$
$$D_{zy} = \frac{d^2}{\left(\frac{1-\nu_{xy}\nu_{yx}}{E_y t}\right)_t + \left(\frac{1-\nu_{xy}\nu_{yx}}{E_y t}\right)_b} \qquad [3.4]$$

3.1.2 Local Instability Failure Modes

3.1.2.1 Face dimpling

Face dimpling or intercellular buckling is a local instability failure where a face sheet buckles within the some limited number of cells of honeycomb or corrugated core. For square cell honeycomb cores face dimpling stress is calculated as follow:

$$\sigma_f = 2,5E_f\left(\frac{t_f}{a}\right)^2 \quad \text{for } \nu=0,3 \qquad [3.5]$$

where a is the length of the side of a cell. For hexagonal honeycombs:

$$\sigma_f = \frac{2E}{1-\nu_f^2}\left(\frac{t_f}{s}\right)^2 \qquad [3.6]$$

where "s" is the radius of circle, tangent inside the walls of a honeycomb cell. For sandwich beams Poisson's ratio in above formula is taken as zero.

3.1.2.2 Face wrinkling

In order to determine critical face wrinkling stress some methods such as energy method and differential equation method have been suggested [27, 28].

Critical stress can be predicted for sandwich panels by the following conservative formulas [4]:

$$\sigma_{fx} = 0,5\sqrt{E_{fx}E_{cx}G_{cx}} \quad \text{and}$$

$$\sigma_{fy} = 0,5\sqrt{E_{fy}E_{cy}G_{cy}} \qquad [3.7]$$

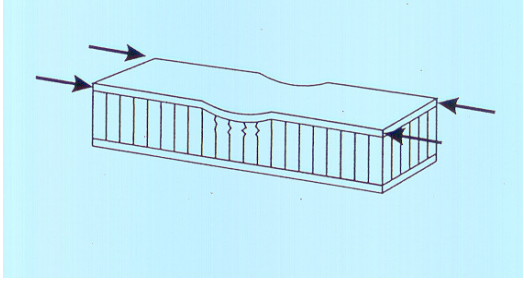

Figure 3.2 Skin wrinkling [54]

3.1.3 General Instability Failure Modes

3.1.3.1 General buckling

This failure type itself does not damage structure but structure must be avoided buckling not to lose its load bearing capacity.

Critical buckling load can be derived analytically as follow [4, 14, 45] for a general case with thick faces;

$$P_{cr} = \frac{\frac{2\pi D_f D}{S(\beta L)^4} + \frac{\pi^2 D}{(\beta L)^2}}{1 + \frac{\pi^2 D}{S(\beta L)^2}} \qquad [3.8]$$

here β depends on the boundary conditions and D is bending stiffness of beam.

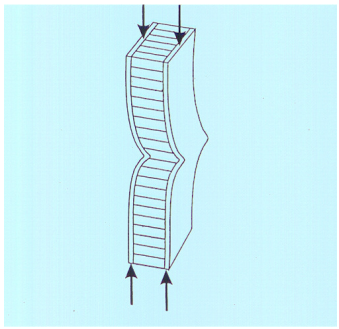

Figure 3.3 General buckling mode of a sandwich beam [12]

3.1.3.2 Core shear crimping

The core thickness and shear modulus must be adequate to prevent the core from failing in shear under edgewise compressive loading.

Shear crimping failure happens as a result of large out-of-plane deformations in a post-buckled state when the transverse forces build up due to the deformation. Failure will happen where the transverse shear force has a maximum.

The critical face stress is for any in-plane direction and lower or bottom face as follow;

$$\sigma_s = \frac{S}{2t_f} \qquad [3.9]$$

3.2 Failure Theories for Analyzing Single Ply Laminate

Failure theories usually investigate the fail mechanisms of a laminated composite ply by ply and often in plane stress conditions. There are not certain analytical methods showing interactions between plies. Recently, Kamoulokos and Kohlgrüber reported a failure model for crash behavior of laminated composites. They modeled laminate discretizing each ply separately. Plies were held together by multipoint constraints or so called spot weld elements. Out of plate failure modes such as delamination growth was predicted based on the forces resulting from the constraints.

For sandwich panels and beams core-face interface behavior is important factor making sandwiches different from laminated plates. However there is not a criteria examining failure mechanisms of core and face sheets together. It is a common way to test failure conditions in core, core-skin interface. The following sections will examine ply base failure criterions which will be considered in design process of this paper. In the Figure below stresses with directions are given required for failure criterions [29].

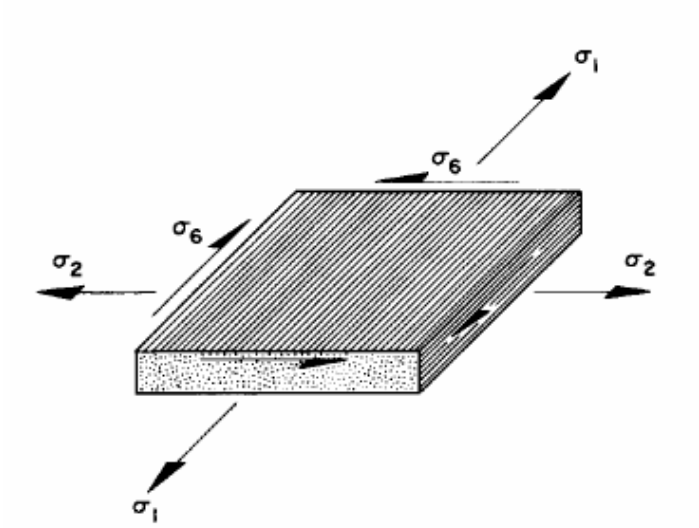

Figure 3.4 An individual layer under plane stress [29]

3.2.1. Maximum Stress Criterion

This criterion is related to the Maximum Normal stress theory by Rankine, Lame and Clapeyron and the Maximum Shear stress theory by Tresca. The stresses acting on a lamina are separated into the normal and shear stresses in the material axes. Layer failure is judged to occur if any of the normal or shear stresses in the material axes are equal to or greater than the corresponding allowable strength values of ply considered.

Failure occurs when;

$$\left.\begin{array}{ll} \sigma_1 \geq \sigma_{1t}^u & or \ -\sigma_{1c}^u \\ \sigma_2 \geq \sigma_{2t}^u & or \ -\sigma_{2c}^u \\ \sigma_6 \geq \tau_6^u & \end{array}\right\} \qquad [3.10]$$

Tensile stresses:

$$\begin{array}{ll} \sigma_1 \geq \sigma_{1t}^u & \text{Fiber Crack} \\ \sigma_2 \geq \sigma_{2t}^u & \text{Matrix Crack} \end{array} \qquad [3.11]$$

Compressive stresses:

$$\begin{array}{ll} \sigma_1 \leq \sigma_{1c}^u & \text{Fiber Crushing} \\ \sigma_2 \leq \sigma_{2c}^u & \text{Matrix yielding} \end{array} \qquad [3.12]$$

Shear stress:

$$|\sigma_6| \geq \tau_6^u \quad \text{Shear Crack} \qquad [3.13]$$

There is no interaction between the stress components.

3.2.2. Maximum Strain Criterion

Criterion is based on maximum normal strain theory by St. Venant and the maximum shear stress theory by Tresca. Likewise, strains applied to a lamina are resolved into the normal and shear strains in the material axes. Failure is judged to occur if any of the normal or shear strains in the material axes are equal to or greater than the corresponding ultimate strains of the ply. Assuming linear relation between stress and strain until failure, allowable or ultimate strains can be found directly from the ultimate strength parameters and elastic modulus. Each strain component is compared with the corresponding ultimate strain. However this theory allows some interactions between stress components because of the Poisson's ratio effect.

Tensile strain:

$$\begin{aligned} \varepsilon_1 &\geq \varepsilon_{1\mathrm{t}}^{\mathrm{u}} \\ \varepsilon_2 &\geq \varepsilon_{2\mathrm{t}}^{\mathrm{u}} \end{aligned} \qquad [3.14]$$

Compressive strain:

$$\begin{aligned} \varepsilon_1 &\leq \varepsilon_{1c}^{\mathrm{u}} \\ \varepsilon_2 &\leq \varepsilon_{2c}^{\mathrm{u}} \end{aligned} \qquad [3.15]$$

Shear strain

$$|\gamma_6| \geq \gamma_6^{\mathrm{u}} \qquad [3.16]$$

or in the terms of stresses, maximum strains;

$$\begin{aligned} \varepsilon_1 &= (\sigma_1 - \nu_{12}\sigma_2)/E_1 \\ \varepsilon_2 &= (\sigma_2 - \nu_{21}\sigma_1)/E_2 \\ \gamma_6 &= \tau_6/G_{12} \end{aligned} \qquad [3.17]$$

Ultimate strains are calculated from uniaxial or shear tests as follow;

$$\begin{aligned} \varepsilon_{1t}^{\mathrm{u}} &= \frac{F_{1t}}{E_1} \text{ and } \varepsilon_{1c}^{\mathrm{u}} = \frac{F_{1c}}{E_1} \\ \varepsilon_{2t}^{\mathrm{u}} &= \frac{F_{2t}}{E_2} \text{ and } \varepsilon_{2c}^{\mathrm{u}} = \frac{F_{2c}}{E_2} \\ \gamma_6^{\mathrm{u}} &= \frac{F_6}{G_{12}} \end{aligned} \qquad [3.18]$$

3.2.3. Tsai-Wu Criterion

Denoting the three shear stresses by $\sigma_4, \sigma_5,$ and σ_6 for the sake of simplicity Tsai-Wu criterion is based on the following function

$$F = F_{ij}\sigma_i\sigma_j + F_i\sigma_i \qquad i, j = 1, 2..., 6 \qquad [3.19]$$

The summation convention for repeated subscript is applied in above expression. According to Tsai-Wu criterion composite ply fails when the following condition is violated

$$F \leq 1 \qquad [3.20]$$

For two-dimensional problems a great simplification can be made as following,

$$F = F_{11}\sigma_1^2 + 2F_{12}\sigma_1\sigma_2 + F_{22}\sigma_2^2 + F_{66}\tau_{12}^2 + F_1\sigma_1 + F_2\sigma_2 \qquad [3.21]$$

In this way, six independent strength properties are required to apply this criterion. Property F_{12} as involved in the interaction term should be determined from a biaxial test. It should be determined from a biaxial test with $\sigma_1 = \sigma_2 = \sigma$. Supposing the material fails at $\sigma = \sigma^*$, then F_{12} is expressed as

$$F_{12} = \frac{1}{2\left(\sigma^*\right)^2}[1 - \sigma^*(F_1 + F_2) - (\sigma^*)^2(F_{11} + F_{22})] \qquad [3.22]$$

Definitions of F_{ij}'s in terms of conventional strength properties;

$$F_{11} = \frac{1}{\sigma_{1t}^*\sigma_{1c}^*} \qquad F_{22} = \frac{1}{\sigma_{2t}^*\sigma_{2c}^*} \qquad F_{66} = \frac{1}{(\tau_{12}^*)^2}$$

$$F_1 = \frac{1}{\sigma_{1t}^*} - \frac{1}{\sigma_{1c}^*} \qquad F_2 = \frac{1}{\sigma_{2t}^*} - \frac{1}{\sigma_{2c}^*} \qquad [3.23]$$

$$F_{12} = \frac{1}{2(\sigma^*)^2}\left[1 - \sigma^*\left(\frac{1}{\sigma_{1t}^*} - \frac{1}{\sigma_{1c}^*} + \frac{1}{\sigma_{2t}^*} - \frac{1}{\sigma_{2c}^*}\right) - (\sigma^*)^2\left(\frac{1}{\sigma_{1t}^*\sigma_{1c}^*} + \frac{1}{\sigma_{2t}^*\sigma_{2c}^*}\right)\right]$$

In absence of biaxial test data, it is sometimes reasonable to assume that, for a unidirectional lamina under an equal biaxial stress state in tension, the lamina would fail at the same stress level as it does under uniaxial transverse tension ($\sigma^* = \sigma^*_{2t}$).

$$F_{12} = \frac{1}{2(\sigma^*_{2t})^2}\left[1 - \sigma^*_{2t}\left(\frac{1}{\sigma^*_{1t}} - \frac{1}{\sigma^*_{1c}} + \frac{1}{\sigma^*_{2t}} - \frac{1}{\sigma^*_{2c}}\right) - (\sigma^*_{2t})^2\left(\frac{1}{\sigma^*_{1t}\sigma^*_{1c}} + \frac{1}{\sigma^*_{2t}\sigma^*_{2c}}\right)\right] \qquad [3.24]$$

3.3 Choice of Criterion in Design

Use of a criterion is usually limited with data obtained for the material [14, 29]. In conventional engineering design problems generally maximum stress and maximum strain criterions are preferred due to the simplicity of calculations. However for the more complex problems, for example fracture or crash modeling of materials, a simple interactive criterion has an advantage to predict element failure of material more accurately than maximum stress or strain criterions.

4. DESIGN OF CABIN FLOOR

4.1 General Considerations

The limitations in vertical impact crashworthy designing of a general helicopter structure were defined in MIL-STD-1290A [2]. Detailed study must be performed in cockpit airframe design. Body frame design is important step for maintain structural integrity during crash simulation. Also, structural integrity of cockpit airframe must be sustained during the crash for occupant safety. Roof panels that carry the heavy machinery must be supported with sufficiently to maintain safe volume for occupants. Body airframes must be stiff enough to transmit loads of heavy machinery to the cabin-floor structure and skids.

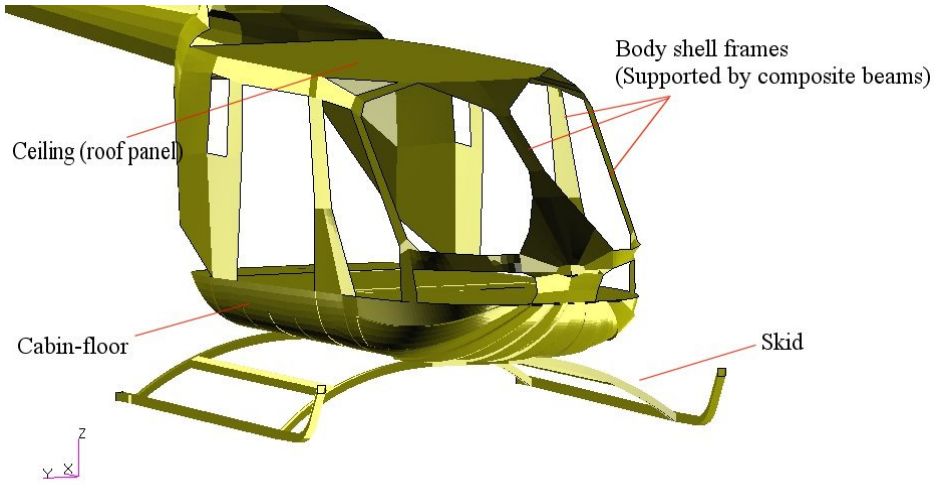

Figure 4.1 Structural components of helicopter

Cabin floor structure must be designed considering safety of fuel tanks. It must absorb significant energy during higher impact velocities than estimated protecting structural integrity as much as possible. It must be rigid enough to prevent possible firing situations caused by fuel system.

Vertical acceleration values considered in the point mass must be lower than the human body limits [30-32] in vertical direction as in Figure [4.1]. Output values do not include seat contribution to absorb deceleration. Therefore predicted seat contribution will be added to output values of vertical acceleration of that point [32].

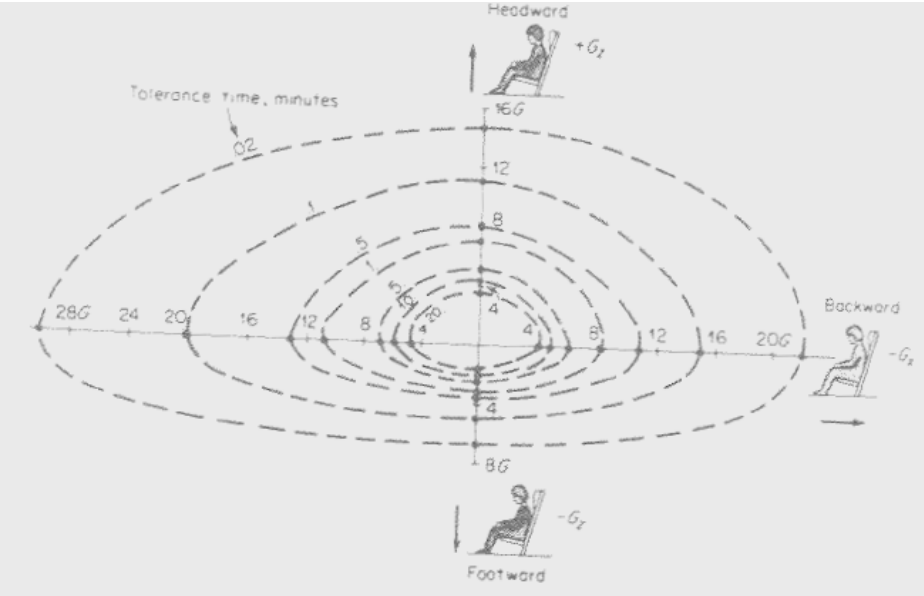

Figure 4.2 Human body acceleration limits [32]

4.2 Loading Schemes and Scenarios

All nodes of model were subjected to initial velocity components defined as in Table 4.1. Vertical velocity and acceleration values were used in crash analysis.

Table 4.1 Crash impact design conditions [2]

Condition Number	Impact Direction	Object Impact	Velocity Change ΔV m/s
1	Longitudinal (Cockpit)	Rigid vertical barriers	6,1
2	Longitudinal (Cabin)		12,2
3	Vertical	Rigid Horizontal Surface	12,8
4	Lateral Type I		7,62
5	Lateral Type II		9,14
6	Combined High angle & vertical	Rigid Horizontal Surface	12,8
	Longitudinal		8,23
7	Combined Low angle & Vertical	Plowed Soil	4,26
	Longitudinal		30,5

4.3 Stipulated Failure Sequence

Energy absorbing sequence is important and it must be considered in design process. Skids of helicopter are to be considered an energy absorbing part of whole structure. It reduces the inertia loads in both vertical and longitudinal directions during impact with ground. When they are failed and not carrying loads anymore then strain energy density will increase rapidly in sub-floor structural elements. Minimum weight and recoverable failure of sub-floor elements was preferred in design methodology [37-39].

4.4 Choice of the Materials and the Material Models for FEA

Each face-sheet of sandwich elements was modeled as 2D orthotropic. Orthotropic materials which have equal tensile and compressive ultimate stresses modeled together with Tsai-Hill failure criteria. Tsai-Wu failure criteria introduced materials which have different strength values in different directions. Core materials were modeled with orthotropic linear elastic material properties. In plane shear modulus G_{12} assumed so higher compared with through thickness shear modulus G_{13}, and G_{23} for face-sheet materials. For honeycomb cores G_{13} and G_{23} are rather greater than in plane shear modulus G_{12}. In the core material models these properties are introduced to model transverse shear deformation of core so that the sandwich effect was modeled. Kevlar clothes were chosen as face-sheet material in most of the cabin-floor elements and in bottom plate because of their superior impact strength values. Honeycomb core materials were used because of their outstanding transverse rigidity and energy absorbing ability during crush events. In transverse and longitudinal stiffeners' face-sheets ±45 stacked plies were used against compressive edgewise reaction forces. Table below shows material models can be used in engineering designs. For orthotropic plies, number of properties can be reduced to four because of plane stress behavior of each individual ply.

Table 4.2 Material models

Material	Symmetry	Constants	Properties
Isotropic	∝ planes	2	E, G (E, ν) (ν, G)
Transversely Isotropic	1 axis	6	E_1, E_2, G_{12}, G_{23}, ν_{12}, ν_{23}
Orthotropic	3 planes	9	E_1, E_2, E_3, G_{12}, G_{13}, G_{23}, ν_{12}, ν_{13}, ν_{23}
Orthotropic Plane element		Important: 4 Negligible: 5	E_1, E_2, G_{12}, ν_{12} E_3, G_{13}, G_{23}, ν_{13}, ν_{23}
Anisotropic	None	21	

4.5 Modelling Overviews of Cabin Floor

Following the structural needs whole helicopter body is mainly constructed with sandwich elements. Cabin floor includes tapered like rectangular composite beam with filled inside structural foam. Bottom of cabin floor is considered as honeycomb core sandwich shell. Floor vessel is supported mainly as transverse bulkheads. Longitudinal supports between bulkheads are assumed to be carried by transverse members. This idea is also important in manufacturing sequence. Some simple structural members were used considering manufacturing capabilities. Engineering assumptions were made to avoid geometrical complexity within the tolerance. Accommodation floor is also designed with sandwich shells.

4.6 FE Modeling of Structure

All body structure is mainly designed with sandwich elements. Face-sheet materials are linear orthotropic elastic composite clothes oriented 0, 45, 90 directions. Non-symmetric sandwich face-sheets were avoided. Face-sheets of sandwich beams and panels were modeled with quadratic 4-nodes shell elements [35, 36] to avoid excessive computation time. Concentrated masses have been connected to cabin-

floor and body model with beam elements with rigid boundary conditions (RBE2) in MSC.DYTRAN (see Figure 4.2, 4.3). The pilot and seat was modeled with point mass elements and resulting vertical acceleration and force values have been requested for these point elements.

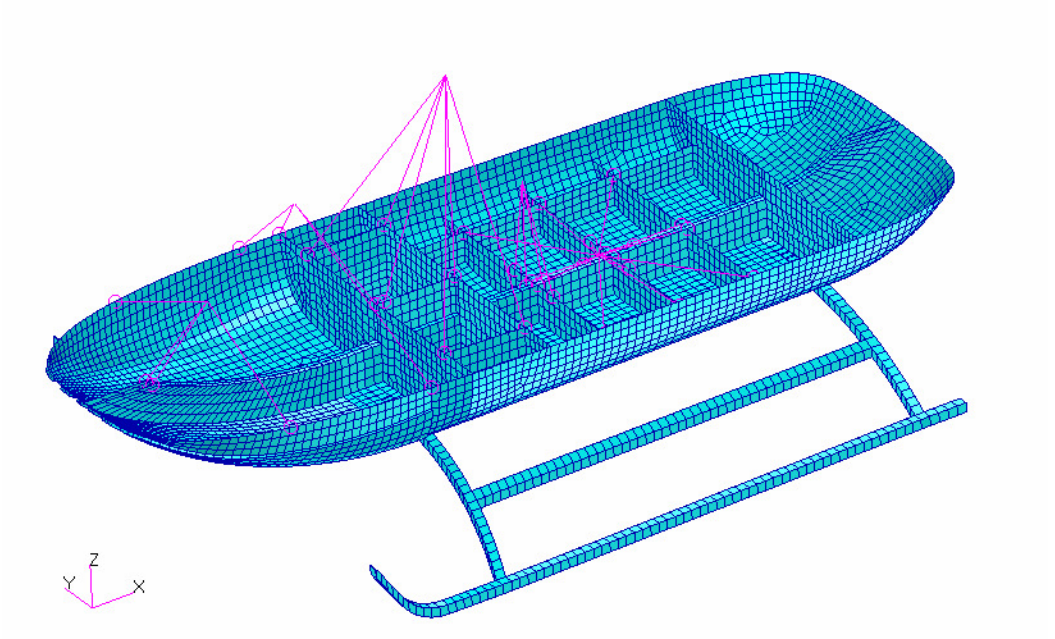

Figure 4.2 Cabin-floor components and point masses

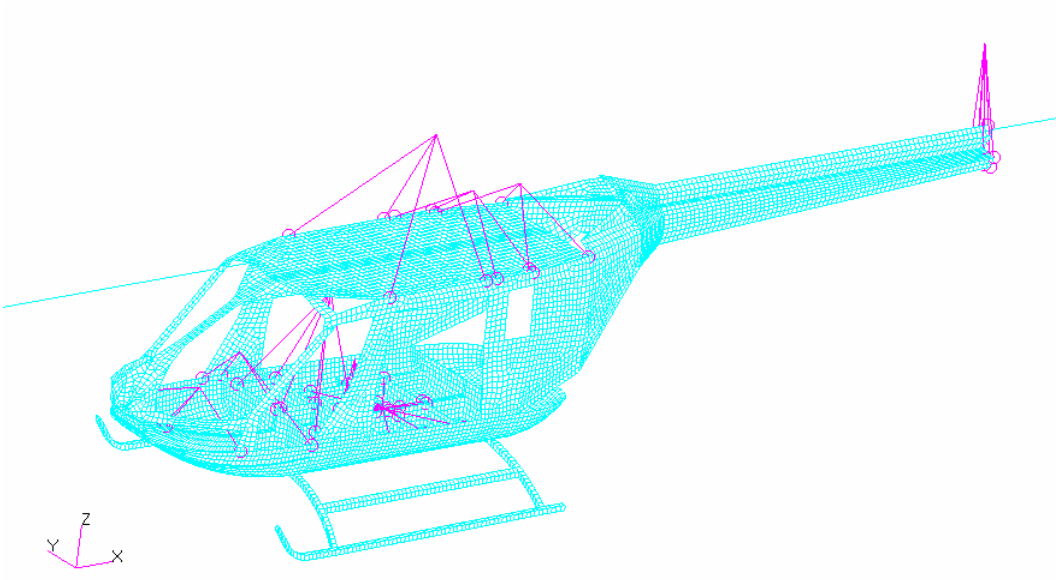

Figure 4.3 Helicopter body model with mass points

Some failure criterion (Tsai-Hill and Tsai-Wu) was used to model onset of failure in each ply. Failure propagation was modeled by removing failed elements from the model at each time step and degrading the model for next time step solution. This approach was used to model global failure of element skins.

Local failures under compressive loading of sandwich elements were examined from the maximum stress outputs of elements. These outputs were used to predict compressive failure modes both local and globally mentioned previously.

Crash simulation has been ended when the total element distortional energy was the stable in condition.

4.7 The Central Difference Method

Equation of motion for finite element system can be written as following form:

$$\mathbf{M}\ddot{x} + \mathbf{C}\dot{x} + \mathbf{K}x = \mathrm{R} \qquad [4.1]$$

where M, C, and K are the mass, damping and stiffness matrices, R is the external load vector and $x, \dot{x}, \ddot{x}$ are the displacement, velocity and acceleration vectors of the finite element assemblage. The central difference scheme assumes the acceleration vector as:

$$\ddot{x}_{\mathrm{t}} = \frac{1}{\Delta t^2}\{x_{\mathrm{t-\Delta t}} - 2x_{\mathrm{t}} + x_{\mathrm{t+\Delta t}}\} \qquad [4.2]$$

and velocity vector as;

$$\dot{x}_{\mathrm{t}} = \frac{1}{2\Delta t}\{-x_{\mathrm{t-\Delta t}} + x_{\mathrm{t+\Delta t}}\} \qquad [4.3]$$

The displacement solution for time $t + \Delta t$ is obtained by considering Equation [4.1] at time t, i.e.,

$$\mathbf{M}\ddot{x}_{\mathrm{t}} + \mathbf{C}\dot{x}_{\mathrm{t}} + \mathbf{K}x_{\mathrm{t}} = \mathrm{R}_{\mathrm{t}} \qquad [4.4]$$

Substituting the relations for $\ddot{x}$ and $\dot{x}$ in [4.2] and [4.3] into the [4.4], leads

$$\left(\frac{1}{\Delta t^2}\mathbf{M} + \frac{1}{2\Delta t}\mathbf{C}\right)x_{\mathrm{t+\Delta t}} = \mathrm{R}_{\mathrm{t}} - \left(\mathbf{K} - \frac{2}{\Delta t^2}\mathbf{M}\right)x_{\mathrm{t}} - \left(\frac{1}{\Delta t^2}\mathbf{M} - \frac{1}{2\Delta t}\mathbf{C}\right)x_{\mathrm{t-\Delta t}} \qquad [4.5]$$

from which $x_{\mathrm{t+\Delta t}}$ can be solved. Solution of $x_{\mathrm{t+\Delta t}}$ is based on using the equilibrium conditions at time t. For this reason the integration procedure is called an explicit

integration method, and such integration schemes do not require a factorization of the global stiffness matrix in the step-by-step solution. Calculation of $x_{t+\Delta t}$ involves x_t and $x_{t-\Delta t}$. Therefore to calculate the solution at time Δt, a special starting procedure must be used. Since x_0, $\dot{x}_0$, and $\ddot{x}_0$ are known, the relations [4.2] and [4.3] can be used to obtain $x_{-\Delta t}$;

$$x_{-\Delta t}^{(i)} = x_0^{(i)} - \Delta t \dot{x}_0^{(i)} + \frac{\Delta t^2}{2} \ddot{x}_0^{(i)} \qquad [4.6]$$

where the superscript (i) indicates the ith element of the vector considered.

5. NUMERICAL RESULTS AND DISCUSSIONS

The following figures were taken from the point element modeling the center of gravity of the pilot. The main indicator for the safe structure is vertical acceleration peak values resulted in crash event. Duration of peak values are very important because they determine whether pilot body will harm or not. Figure 4.2 shows a human body acceleration limits in different directions.

In Figure 5.1, vertical acceleration values were shown in mm/s^2 unit. Converting acceleration values in the following figures to compact unit "g" dividing 10^4, will give values to compare with human body limits. The peak value occurred at 0,006 second after sub-floor elements started contact with rigid ground. After this moment, heavy equipments and machinery forced structure to deform continuously. Stress waves moved through the structure rapidly and caused the structural elements fail. The fluctuation in acceleration graphics means that helicopter body oscillates in vertical direction by reaction force motions through the body causing various stress environments on structural elements. This causes many body elements to fail after crash. Figure 5.2 shows failed elements after peak value of impact.

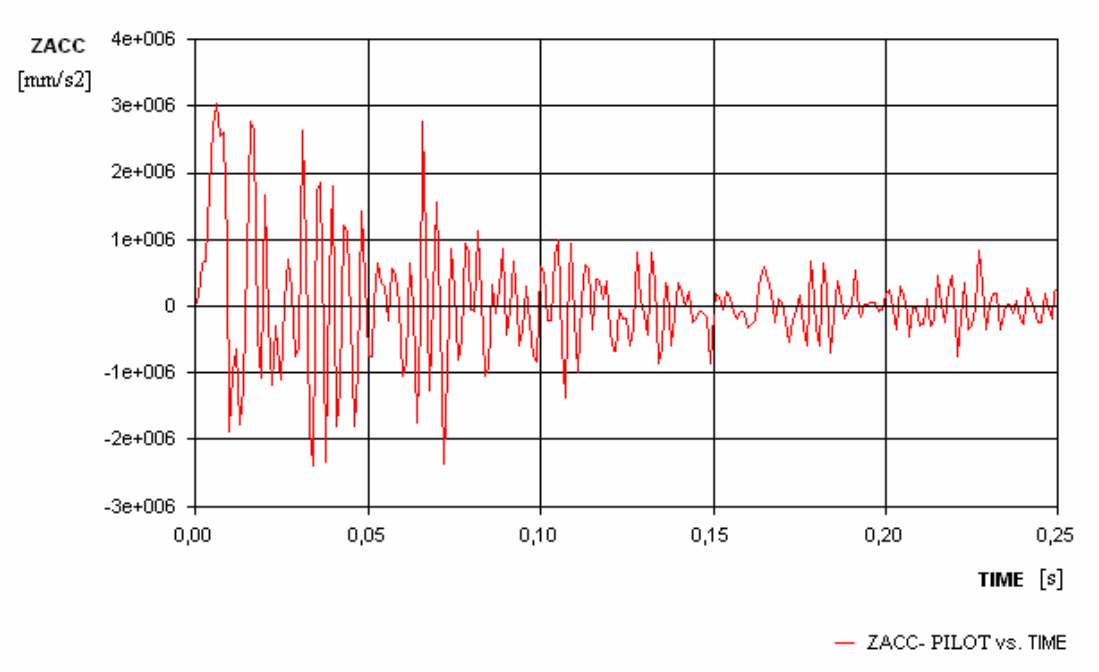

Figure 5.1 Vertical accelerations of point element modeling pilot

MSC.DYTRAN has an option to remove failed elements from the structure. Figure 5.2 shows failed elements just after the crash event. This analysis was performed according to rules for retracted gear model expressed in related reference [2].

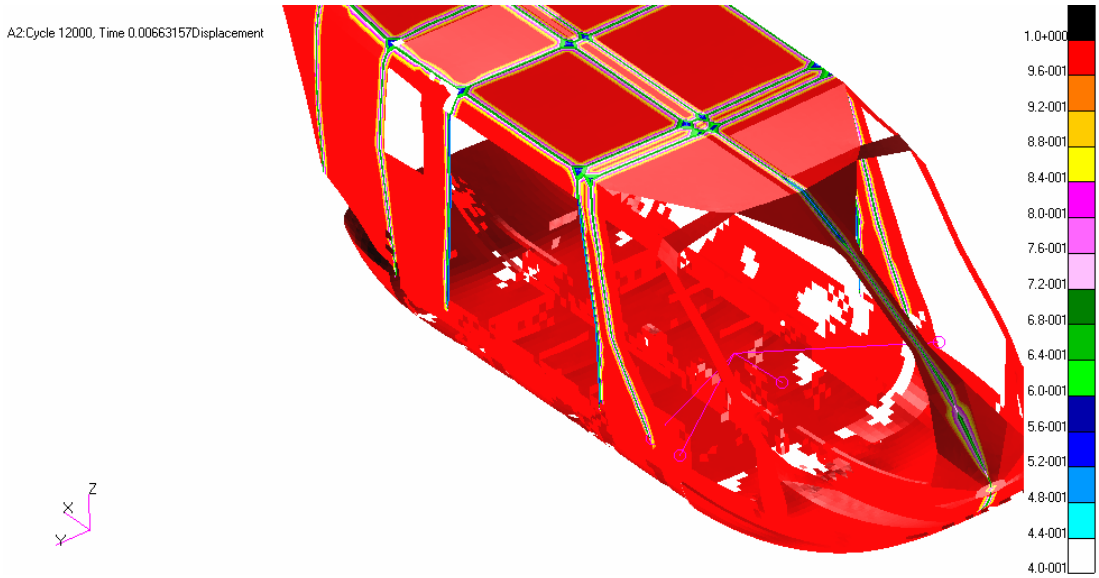

Figure 5.2 Failed elements just after crash impact

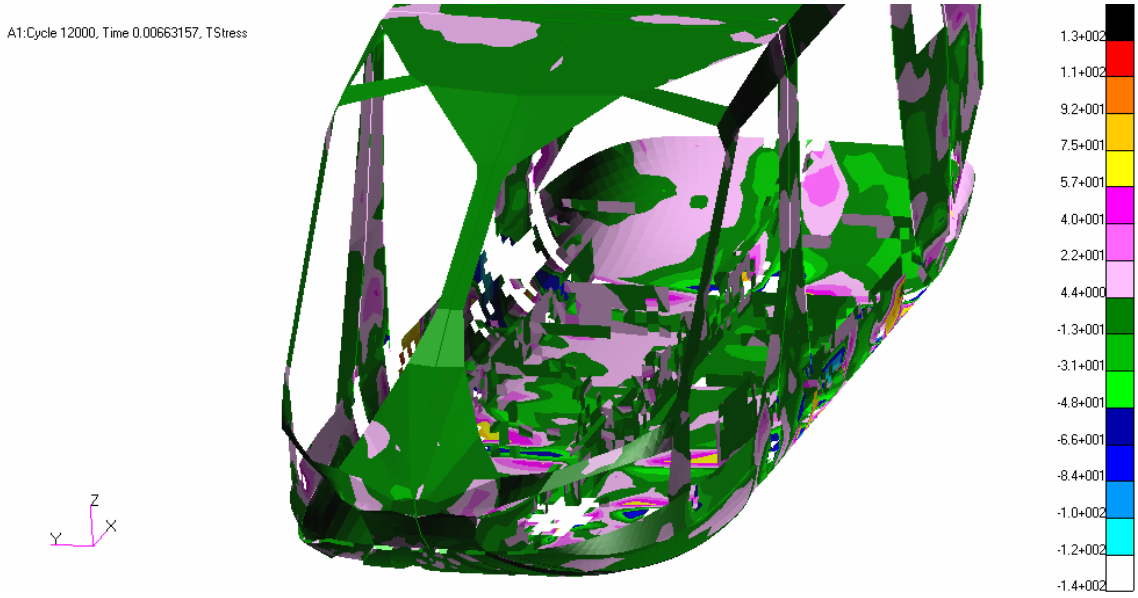

Figure 5.3 In-plane shear stress distribution just after crash impact

The velocity graph in Figure 5.4 shows that after crashing, point element modeling pilot loses it top speed in 0,05 second. And also acceleration data show that pilot is under high acceleration in 0,04 second duration. Endurance limits of human body allow just over 8g in vertical directions. But these values are lofty than limits of bodies. In this model, point elements which model the concentrated masses are

linked to the structure with rigid beam elements. Therefore any resulted force from impact of body directly arrives to these point elements without any absorption. This is worst case scenario. In real these concentrated masses are in relation with body with a wide surface or they are subparts of body. For the sake of simplicity they are not modeled as they are in real.

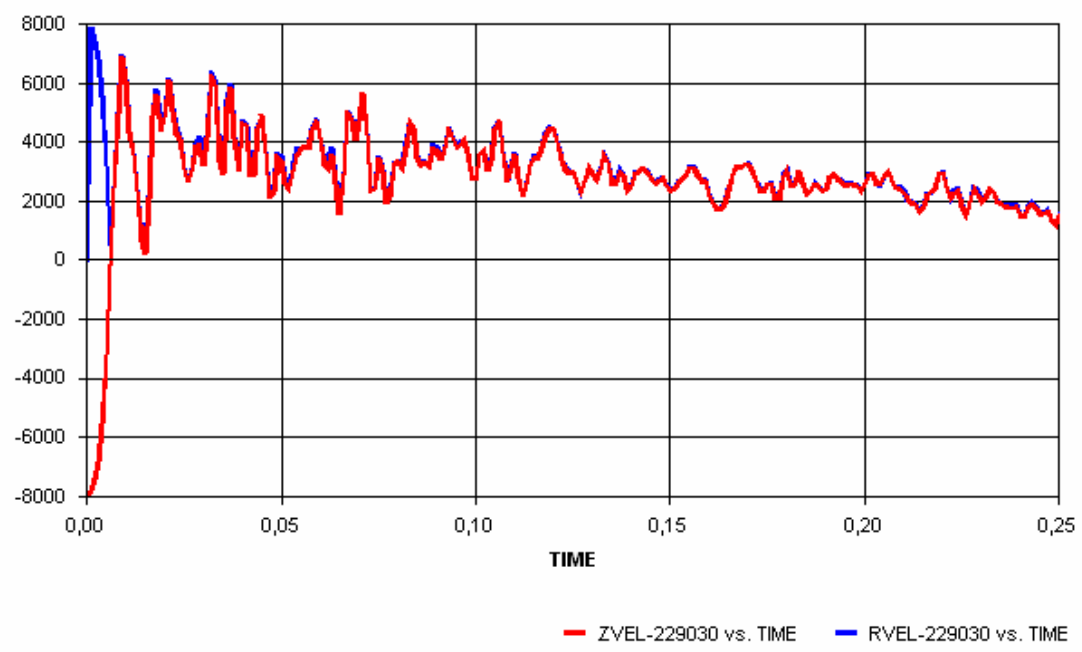

Figure 5.4 Velocity change of point element modeling pilot

Thus resulting forces will be transmitted being separated more than one node and the values will be in less level in real case. This will reduce the acceleration outputs values of nodes (grid points).

6. RECOMMENDATIONS FOR FUTURE STUDY

Through this paper a preliminary design from sandwich elements were examined to meet crashworthy capability of sub-floor structure. Material nonlinearity was not introduced to model. However; materials used in the model such as Kevlar® and S-Glass show extraordinary dynamical strength under permanent and combined loading conditions. Only linear properties from the uni-axial and bi-axial tests of composite elements were used and introduced to a properly chosen failure criteria. Therefore materials were modeled as if they have a conservative contribution to the overall strength and energy absorbing behavior. The reason of using linear elastic properties is common one. It is hard to obtain dynamical properties of such materials somehow without testing. But there are some common properties datasheets for known materials and as an extent they give ideas about the materials.

Crash environment was idealized using flat and rigid surface ground for the sake of simplicity in model. However; it is necessary to examine in different type of landing conditions and ground types. But this is a future study and needs a series full scale tests with different ground conditions such as soil, asphalt, and concrete.

Effects of joints and sub-elements were neglected. Therefore; localized effects due to joints were missed in model and it is also a detail job for this study.

Designing a crashworthy philosophy is a complex phenomenon. Before all, it is needed to be understood how the stresses propagate through the elements designed during crush time interval step by step. Then it is required to create a special design for critical places where the stress intensity is increased rapidly. Through this paper first step is examined, so following designs will be for the special crashworthy purposes.

Especially in composite design first manufacturing method is important. The same reinforcement material can have different mechanical properties in composite state when it is manufactured by different techniques. So reinforcement choice and proper manufacturing method must be decided before design works.

REFERENCES

[1] Fleming, D.C., "Delamination Modeling of Composites for Improved Crash Analysis", FL, USA

[2] MIL-STD-1290A, Light fixed and rotary-wing aircraft crash resistance, Department of Defense, USA

[3] Allen, G.H., 1969, "Analysis and design of structural sandwich panels", Pergamon Press

[4] Zenkert, D., 1997, "An introduction to Sandwich Construction", *E-MAS Publishing*

[5] Fasanella, L., Jackson, K.E., Lyle, K.H., 2004, "Multi-Terrain Impact Testing and Simulation of a Composite Energy Absorbing Fuselage Section", *US Army Research Laboratory*, Hampton, VA

[6] Fleming, D.C., "Modeling Delamination Growth in Composites using MSC.Daytran", FL, USA

[7] Majamäki, J., "Impact Simulations of a Composite Helicopter with MSC.Dytran" Eurocopter Deutschland

[8] Vicente, J.L.S., Beltran, F., Martinez, F., 2000, "Simulation of Impact on Composite Fuselage Structures", *ECCOMAS*, Spain

[9] Bisagni, C., 1999, "Crashworthiness of helicopter subfloor structural components", Aircraft Engineering and Aerospace Technology: An International Journal, Vol71 6-11

[10] Johnson, A.F., Lützenburger, M., "HeliSafe: Improved Occupant Crash Safety in Helicopters", DLR, Stutgart, Germany

[11] ANSYS ® Element Reference

[12] Hexcel Sandwich Handbook, available at www.hexcelcomposites.com

[13] Timoshenko, S., Woinowsky-Krieger, S., 1959, "Theory of plates and shells", McGraw-Hill

[14] ASM Handbook, Vol.21 Composites, 2001

[15] Shenoi, R.A., Groves, A., Rajapakse, Y.D.S. 2005, "Theory and Applications of Sandwich Structures", *Southampton University Press*, GB, [pps.267-284]

[16] Staab, G.H., 1999, "Laminar Composites", Butt.- Hein., USA

[17] Matthews, F.L., Davies, G.A.O., Hitchings, D., Soutis, C., 2000, "Finite Element Modelling of Composite Materials and Structures", CRC Press, Boca Raton, USA

[18] Nettles, A.T., 1994, "Basic Mechanics of Laminated Composite Plates", NASA Reference publication, 1351, MSFC, AL, USA

[19] Rabinovitch, O., Frostig, Y., 2001, "High-Order Analysis of Unidirectional Sandwich Panels with Flat and Generally Curved Faces and a "Soft" Core", *Journal of Sandwich Structures,* **3,** 89-116

[20] Shi-Dong Pan, Lin-Zhi Wu, Yu-Guo Sun, Zheng-Gong Zhou, Jia-Lin Qu, 2004, "Longitudinal shear strength and failure process of honeycomb cores", *Composite Structures,* **72,** 42-46

[21] Olsson, R., 2002, "Engineering Method for Prediction of Impact Response and Damage in Sandwich Panels", *Sandwich Structures and Materials*, **4**

[22] Yang, M.Y., Huang J.S., 2005, "Elastic buckling of regular hexagonal honeycombs with plateau borders under biaxial compression", *Composite Structures J*., **71**, 229-237

[23] Gdoutos, E.E., Pilakoutas, K., Rodopoulos, C.A., 2000, "Failure Analysis of Industrial Composite Materials", McGraw-Hill, USA

[24] http://www.marinecomposites.com, last visited 02.22.2006

[25] Mamalis, A.G., Manolakos, D.E., Ioannidis, M.B., Papapostolou, D.P., 2005, "On the crushing response of composite sandwich panels subjected to edgewise compression: experimental", *Composite Structures J*., **71**, 246-257

[26] Kulkarni, N., Mahfuz, H., Jeelani, S., 2004, "Fatigue Failure Mechanism and Crack Growth in Foam Core Sandwich Composites under Flexural Loading", *Reinforced Plastics and Composites J*., **23 1/2004**

[27] Fagerberg, L., Zenkert, D., 2005, "Effects of Anisotropy and Multiaxial Loading on the Wrinkling of Sandwich Panels", *Sandwich Structures and Materials,* **7,** 177-194

[28] Rey, L.P., Lin, W., Mbanefo, U., 1999, Facesheet wrinkling in sandwich structures, Northrop Grumman Corporation, El Segundo, CA, USA

[29] ESDU DATA ITEM, "Failure Analysis of Fiber Reinforced Composite Laminates"

[30] Helicopter seat design limits injuries during crashes available at: http://www.csir.co.za/plsql/ptl0002/PTL0002_PGE038_ARTICLE?ARTICLE_NO=4690137, Last visited 03.23.2006

[31] Sanders, M.S., McCormick, E.J., (1992), Human Factors in Engineering and Design, McGraw-Hill

[32] Crawford, H., 2003, "Survivable Impact Forces on Human Body Constrained by Full Body Harness"

[33] Gan, C., Gibson, R.F., Newaz, G.M., 2004, "Analytical/Experimental Investigation of Energy Absorption in Grid-Stiffened Composite Structures under Transverse Loading", *Experimental Mechanics,* **44,** 185-194

[34] Gibson, R.F., 2005, "Energy absorption in composite grid structures", *Adv. Composite Mater.*, **14**, 113-119

[35] ESI-GROUP PAM-CRASHSAFE Reference Manual (2004)

[36] MSC.DYTRAN User Manuals

[37] Jackson, K.E., 2000, "Impact Testing and Simulation of a Crashworthy Composite Fuselage", *US Army Research Laboratory*, Hampton, VA

[38] Kim, H.S., Wierzbicki, T., 2001, "Crush behavior of thin walled prismatic columns under combined bending and compression", *Pergamon Press*, USA

[39] Gan, C., 2003, "Behavior of Grid-Stiffened Composite Structures under Transverse Loading", *PhD Thesis*, Wayne State Univ., Detroit, MI

[40] Gay, D., Hoa, S.V., Tsai, S.W., 2003, "Composite Materials Design and Application", CRC Press LLC, Boca Raton, USA

[41] http://www.baltek.com, Last visited 01.30.2005

[42] DIAB GROUP INC., http://www.diabgroup.com/europe/products/e_prods_2.html, last visited 01.20.2006

[43] Tay, T.E., Tan, V.B.C, Deng, M., (2003), "Element-failure concepts for dynamic fracture and delamination in low-velocity impact of composites", International Journal of Solids and Structures, **40** 555-571

[44] Gibson, R.F., 1994, "Principles of Composite Material Mechanics", McGraw-Hill

[45] Vinson, J.R., 1999, "The behavior of sandwich structures of isotropic and composite materials", Technomic Publication

[46] Reddy, J.N., 2004, Mechanics of Composite Laminated Plates and Shells: Theory and Analysis, Second Edition", CRC Press LLC, Boca Raton, USA

[47] Kim, J.K., Yu, T.X., 1998, "Impact Response and Dynamic Failure of Composites and Laminate Materials Part 2: Strain-Rate Effect, Energy Absorption and Modeling", Trans Tech Pub., Swiss

[48] Sharma, S.C., Murthy, N., Krishna, M., 2004, "Interfacial studies in Fatigue Behavior of Polyurethane Sandwich Structures", *Journal of Reinforced Plastics and Composites,* **23,** 893-903

[49] Bakis, C.E., 2003, "Composite Materials: Testing and Design, Fourteenth Volume", ASTM Int., USA

[50] Karakuzu, R., Gülem, T., İçten, M., 2006, "Failure Analysis of woven laminated glass-vinylester composites with pin-loaded hole", *Composite Structures,* **72,** 27-32

[51] Fasanella, L., Jackson, K.E., 2003, "Water Impact Test and Simulation of a Composite Energy Absorbing Fuselage Section", *US Army Research Laboratory*, Hampton, VA

[52] Joint Aviation Authorities, 2002, JAR-27 Small Rotorcraft

[53] Reddy, J.N., Wang, C.M., Wang, C.Y, 2005, "Exact Solutions for Buckling of Structural Members", CRC Press LLC, Boca Raton, USA

[54] http://www.hexcel.com/Products/Downloads, last visited 02.12.2005

[55] http://www.euro-composites.com/frames/hintergrund-e.htm, Last visited 01.30.2005

APPENDIX A

SANDWICH ELEMENTS

Core Materials

Honeycombs: They are anisotropic in nature, used in sandwich structures as core material in generally aerospace structures. Honeycomb shows extremely high strength and flexural rigidity in thickness direction in both tensile and compressive forces.

In other directions, it has weaker properties but still good for shear strength. For regular cell shaped honeycombs shear strength values are generally close to each other. Honeycomb cores make the structure more strong in crush event and have significant energy absorbing capabilities. They can be produced in different shapes and with different materials such as kraft paper, aluminum, steel, fiberglass, carbon etc. depending on application area. Hexagonal cell shape gives minimum density for a given material amount of material.

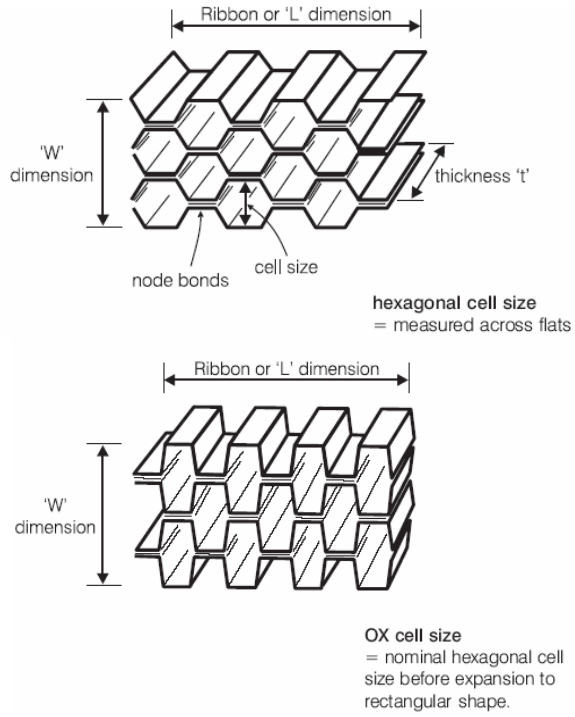

Figure A.1 Example of some honeycomb cell shapes [40]

Balsa: Balsa is a natural wood product and shows a typical core material behavior. In fiber direction it has very good compressive and tensile strength properties. However; it is not so much good in shear strength as to be in honeycombs in the planes perpendicular to fiber direction. It is restricted in use in some cases because of moisture problem. Generally they are used as separate blocks assembling a plane sheet grid to prevent moisture propagation. They are about a half dense of other common woods but denser than corrugated cores. Less than 100 kg/m^3 in dense is not available for balsa wood.

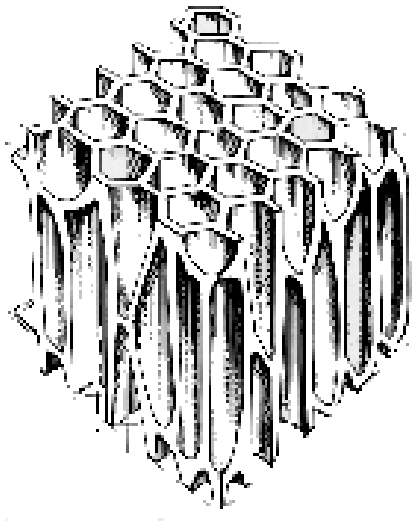

Figure A.2 Structure of balsa wood [41]

Foams: In composite structures foams are used either a former or a structural component. Most general foams are polyurethane and polyvinyl chloride (PVC) foams in composite structures. They are assumed isotropic in mechanical behaviors. To 80C they are used but lose their mechanical properties dramatically at these temperature values.

Figure A.3 Flat sheet/grid scored structural foams from Divinycell [42]

RESUME

I was born in 1980 in Bursa. I completed my primary and secondary education in different cities. I graduated from high school in 1997 then I started my university education at Mechanical Engineering Faculty of Istanbul Technical University. I graduated in 2003 as mechanical engineer and immediately I began my M.Sc. education in Solid Mechanics Program of ITU Institute of Science and Technology.

In my second year of M.Sc. education, I studied in a shipyard company as structural design chief of high speed low craft composite patrol boats.

I am interested in mechanics of composite sandwich materials, computational mechanics, design of crashworthy and lightweight structures and FEM in engineering.